International Journal of Science and Engineering Applications (IJSEA)
Volume 2 Issue 4, 2013, ISSN - 2319-7560 (online)

WSN Based Air Pollution Monitoring System

Amol R. Kasar
Department of Computer Engg,
MIT Academy Of Engg.
Pune University,
Pune,India

Dnyandeo S. Khemnar
Department of Computer Engg,
MIT Academy Of Engg.
Pune University,
Pune, India

Nagesh P. Tembhurnikar
Department of Computer Engg,
MIT Academy Of Engg.
Pune University,
Pune, India

Abstract: Air pollution monitoring is extremely important as air pollution has a direct impact on human health and environment. In this paper we introduce a wireless sensor network system for participatory air pollution monitoring. The traditional air quality monitoring system, controlled by the Pollution Control Department, is extremely expensive. Analytical measuring equipment is costly, time and power consuming. In contrast to traditional air pollution monitoring stations, we present the design, implementation, and evaluation of low power, low cost WSN based Air Pollution Monitoring System which provides real time monitoring of polluted materials at proper locations by using distributed (real time) air pollution monitoring systems.

Keywords: Air Pollution, AtMega16 microcontroller, MG811 Sensor ,MQ6 Sensor,MQ135 Sensor, Real Time, ZigBee, WSN

1. INTRODUCTION

Air pollution is one of the most important factors affecting the quality of life and the health of the increasingly urban population of industrial societies. In many cities, the air is polluted by emissions from sources such as cars and trucks, power plants, and manufacturing processes. When gases and particles from those activities accumulate in the air in high enough concentrations, they can be harmful for human health, an environment. Often, terrain and meteorological conditions complicate air quality issues in the area. Although the national trend is toward better outdoor air quality, there are some urban areas in which no improvement has taken place. Concentrations of outdoor air pollutants vary from day-to-day and even during the course of a day.

For health protection, the public needs timely information about air quality and other factors (e.g., weather conditions) that affect it. An access to air quality forecasts allows residents to reduce their exposure when the pollutant concentrations are high. This is important particularly to people who are sensitive to certain pollutants' harmful effects. For example, people with asthma may be sensitive to ground-level ozone and sulphur dioxide. The major motivation behind our study and the development of the system is to help the government to devise an indexing system to categories air pollution in India. The project is to build an air pollution monitoring system, so a detection system for multiple information of environment is designed in this project. This project is built for low cost, quick response, low maintenance, ability to produce continuous measurements. The main goal of this project is to monitor the air pollution, hazardous gases and increase awareness about pollution by using air pollution monitoring system. Present state of the air quality control in almost all industrial centers in our country is based on taking samples one or few times a day, which means that there is no information about time distribution of polluted materials intensity during day. This is the main disadvantage of such system.In the area, there are two methods to use to monitor air pollution at present. The one is passive sampling (nonautomatic), and the other is continuous online monitoring (automatic). The advantage of the passive sampling method lies in that the monitor equipment is simple and inexpensive, but it can only get on-site monitoring parameters in a certain period, cannot provide real-time values. Meanwhile, the results of monitoring effect by the man factor largely and it will seriously damage the health of the monitoring man in the site of high concentration of harmful substances.

The procedure of continuous monitoring method is as follows: use sensors to monitor the parameters, and then send to the control center by network. The way of data transfer include both wired and wireless. The wired way usually uses public telephone network, or fiber-optic to realize data transmission. Although this method is stable and reliable, with high speed of data transmission, but the shortcomings of the method is also obvious in a wide and dynamic range. With the rapid development of communication technology, network technology and remote sensing technology, there is a trend that air pollution monitoring system is often designed in wireless mode. At present, the wireless mode in air pollution monitoring system includes GSM, GPRS, etc. But these modes are high cost in both installation and maintenance, and complexity. In the other hand, Wireless sensor network have been rapidly developed during recent years. Starting from military and industrial controls, its advantages include the liability, simplicity, and low cost. Based on these advantages, it is now being applied in environmental monitoring. In air pollution monitor applications, we have designed a WSN based air pollution monitoring system using ZigBee networks for City. They focus on implementation of air pollution monitoring system, and developed an integrated wireless sensor board which employs CO2, NO2/NH3 temperature sensor, atmega16 micro-controller, database server and a ZigBee module.

2. System Overview

2.1 Proposed System

Figure 1:Proposed system scenario

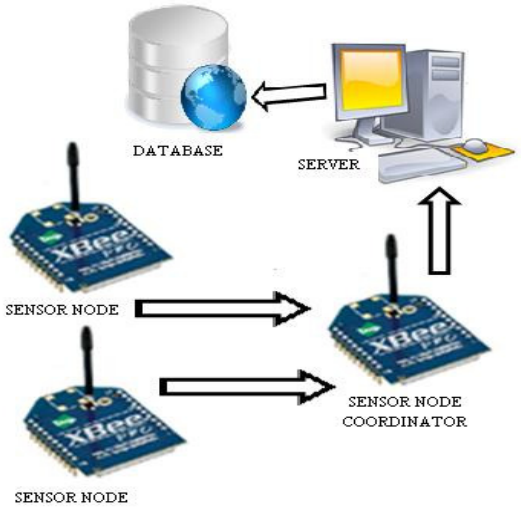

The working of proposed Air pollution monitoring system as follows:

1. Develop architecture to define nodes and their interaction.
2. Collect air pollution readings from a region of interest.
3. Collaboration among thousands of nodes to collect readings and transmit them to a gateway, all the while minimizing the amount of duplicates and invalid values.
4. Use of appropriate data aggregation to reduce the power consumption during transmission of large amount of data between the thousands of nodes.
5. Visualization of collected data from the WSN using statistical and user-friendly methods such as tables and line graphs.
6. Provision of an index to categorize the various levels of air pollution, with associated colors to meaningfully represent the seriousness of air pollution.
7. Generation of reports on a daily or monthly basis as well as real-time notifications during serious states of air pollution for use by appropriate authorities

2.2 Hardware Architecture

The proposed system is designed by integrating the following hardware modules shown in Fig. 2. As the figure shows, the system consists of a ATMEGA16 microcontroller integrated with a sensor array using analog ports. The hardware unit is also connected to a GPS module and a ZigBee-Modem using the RS-232 interface. Each of these components is described in the following

2.2.1. ATMEGA16 microcontroller

The ATMEGA16 microcontroller is the main component of a pollution detection unit. The operating system that runs inside the chip coordinates the substances measurement process, the acquisition of the GPS coordinates and the data transmission

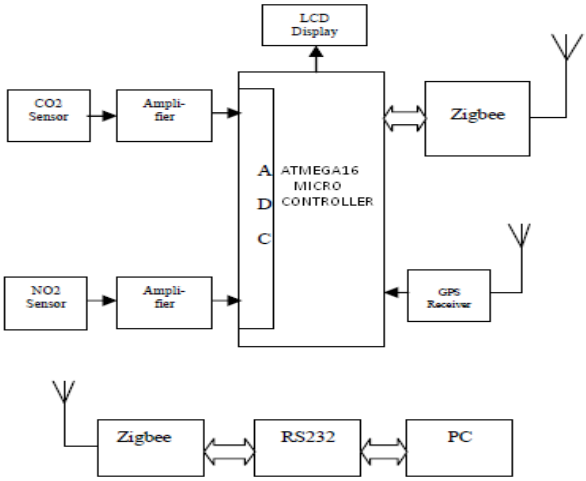

Figure 2: System hardware basic building blocks

to the central server. The microcontroller is mounted on a development board that provides an RS232 serial communication to the ZigBee modem and ZigBee receiver and a parallel connection to the gas sensors. The connection between the gas sensors and the ATMEGA16 microcontroller can't be made directly because of the very small output voltages provided by the sensors (mA).This problem is solved by using auxiliary electronic circuits for signal conversion like OA (*Operational Amplifiers*) and transistors.(see Figure 2)

2.2.2. Sensors Array

The sensor array consists of two air pollutions sensors including Carbon Dioxide (CO2), Nitrogen Dioxide (NO2). As Table I shows, the resolution of these sensors is sufficient for pollution monitoring. Each of the above sensors has a linear current output in the range of 4 mA–20 mA. The 4 mA output corresponds to zero-level gas and the 20 mA corresponds to the maximum gas level. A simple *signal* conditioning circuit is designed to convert the 4 mA–20 mA range into 0–5 V to be compatible with the voltage range of the built-in analog-to digital converter in the ATMEGA16 microcontroller. (see Figure 1,2)

2.2.3. ZigBee Modules

In this paper, two types ZigBee modules are used to organize a network for air pollution monitoring system. The network is controlled by devices called the ZigBee coordinator modem (ZCM). The ZCMs are responsible for collecting data and maintaining the other devices on the network, and all other devices, known as ZigBee end devices (ZED), directly communicate with the ZCM. The ZigBee module is hardware platform of wireless device. The modules realize the basic function of Physical and MAC layer, such as transmit and receive, modulation and demodulation, channel and power control. They operate at 2.4GHz frequency ISM band wireless communication. The modules include a digital direct sequence spread spectrum base band modem and an effective data rate of 250 kbps. They employ the EM2420 2.4GHz radio frequency transceiver and the ATMEL 8-bit AVR microcontroller. They also exhibit a nominal transmit of -1.5dBm and a receive sensitivity of -92dBm When powered at

3.0V, the modules draw 31.0mA in transmit mode and 28mA in receive mode. When the entire module is in sleep mode, the current draw is reduced to approximately 10uA.(see figure 1,2)

Table 1. Sensor Specification

Sensor	C02	N02
Resolution (ppm)	< 1.5	< 0.02
Resp. time (t90)(s)	< 60	< 60
Op. range (ppm)	0-10000	0-20
Operating life (yrs)	>2	>2
Diameter (mm)	20	20

2.3.4. Central Server

The Central-Server is an off-the-shelf standard personal computer with accessibility to the Internet. The Pollution Server is connected to the ZigBee-Modem via RS-232 communication standard. The air pollution information sent from each ZED are collected to ZCM. And then the data are saved to database of central server.(see figure 1)

3. ZigBee Standard

The ZigBee is the new short range, low power, and low data rate wireless networking technology for many applications. It is best specified the bottom three layers (Physical, Data Link, and Network), as well an Application Programming Interface (API) based on the 7-layer OSI model for layered communication systems. Figure-3 shows the layered protocol architecture adopted by the alliance. It should be noted that the ZigBee Alliance chose to use an already existing data link and physical layers specification. These are the recently published IEEE 802.15.4 standards for low rate personal area networks.(see figure 3)

A communication network is composed of many nodes, each of which can transmit and receive data over communication links, wireless or cabled supports network topologies. The ZigBee network layer supports star, tree and mesh topologies. The ZigBee coordinator is responsible for initiating and maintaining the devices on the network, and all other devices, known as end devices, directly communicate with the ZigBee coordinator. In mesh and tree topologies, the ZigBee coordinator is responsible for starting the network and for choosing certain key network parameters but the network may be extended through the use of ZigBee routers. In tree networks, routers move data and control messages through the network using a hierarchical routing strategy.(see figure 4)

The IEEE 802.15.4 standard defines three frequency bands of operation: 868MHz, 916MHz and the 2.4GHZ bands for ZigBee. 2.4GHz bands are used the most commonly available wireless communication products throughout the world because of ISM (Industrial, Scientific, Medical) band. In addition this band offers the highest achievable data rate of 250Kbps and 16 channels between 2.4GHz and 2.4835GHz at the physical layer. Typical transmission distances are within the range from 30 meters in an indoor non-line of sight environment to over 100 meters in a line of sight environment. But problems related a range can be solved through applying routing algorithm at the network layer.(see figure 5)

Figure 3: ZigBee protocol stack for layered wireless communication

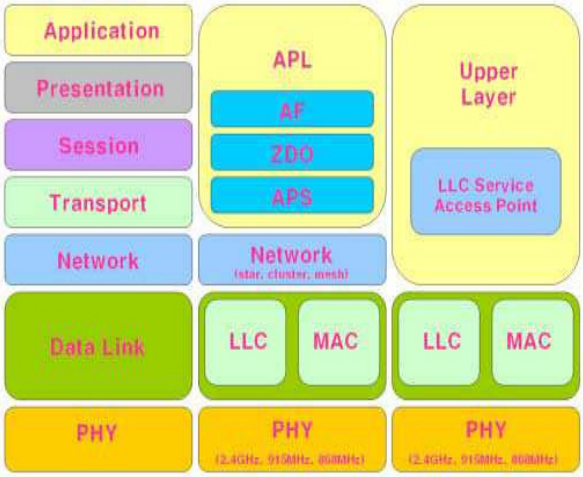

Figure 4: ZigBee network topologies

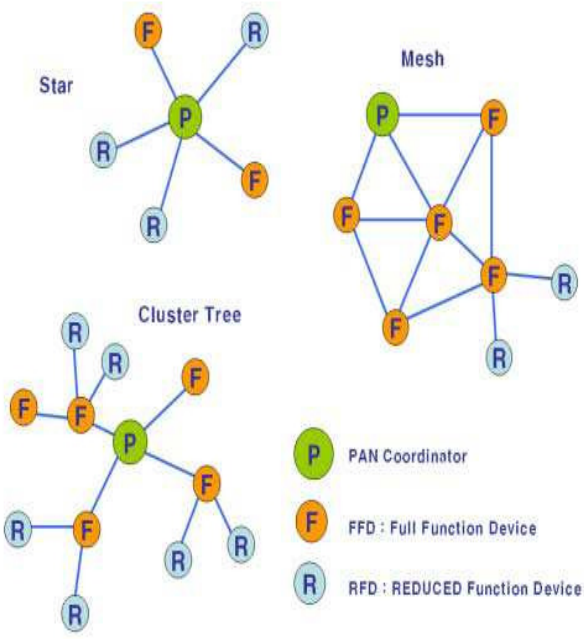

Although defined as 25mW in the world, transmit output power of ZigBee is limited within 10mW. Therefore ZigBee

modules employ dipole type antenna to increase gain of antenna.

Figure 5: Frequency Bands Used for ZigBee

4. AIR Quality

In a general way, it is possible to describe the atmosphere as a very thin gaseous film, where all the meteorological phenomena that regulate the human life occur. Filled with a great diversity of molecules (Table I), the atmosphere performs, at the same time, a role of protection and regulation. Air pollution can have various definitions. According to, "air pollution means the presence, within the external atmospheres, of one or more contaminants, or its combination in quantities or with a temporal duration that can become harmful to human life, vegetable, animal or goods.

The air contaminants include smokes, steams, paper hashes, dusts, soot, carbonic smokes, gases, fogs, radioactive material or toxic chemical products." Certain atmospheric pollutants react with each other creating others pollutants called secondary pollutants. The dissociation, trough the sun's effect, of volatiles organic compounds, carbon monoxide and nitrogen oxide, produced by automobile's motors, lead to the formation of ozone, essentially during the summer, whetemperature reaches higher levels.

Table 2. Average composition of pure air

Element	Symbol	Proportion
Nitrogen	N2	78.084%
Oxygen	02	20.946%
Argon	Ar	0.943%
Carbon dioxide	C02	340 ppm
Neon	Ne	18.18 ppm
Helium	He	5.24ppm
Methane	CH4	1.5 ppm
Krypton	Kr	1.14 ppm
Hydrogen	H	0.50 ppm
Oxide Nitrous	N2O	0.40 ppm
Xenon	Xe	0.09 ppm

Air pollution has dramatic consequences for human health, leading to respiratory problems and even death [6] and for the environment like the greenhouse effect, acid rains and ozone layer reduction.

The European Community has dedicated special attention to the problem of the most representative pollutants concentration, such as the case of Carbon Monoxide (CO), Nitrogen Dioxide (NO2), Sulphur Dioxide (SO2), Ozone (O3) and particles of 10 µm or less (PM10) and special Regulations have been produced. Although the Carbonic Dioxide (CO2) isn't considered a pollutant, its concentration has also to be quantified, due to importance of this gas to the planet's ecosystems.

The system presented here is capable of measuring the following gases in the atmosphere:

4.1 Carbon Dioxide (CO2) – Carbon Dioxide is a gas essential to life in the planet, because it is one of the most important elements evolving photosynthesis process, which converts solar into chemical energy. The concentration of CO2 has increased due mainly to massive fossil fuels burning. This increase makes plants grow rapidly. The rapid growth of undesirable plants leads to the increase use of chemicals to eliminate them.

4.2 Sulphur Dioxide (SO2) – Sulphur Dioxide is a colorless gas, detectable by the distinct odor and taste. Like CO2, it is mainly due to fossil fuels burning and to industrial processes. In high concentrations may cause respiratory problems, especially in sensitive groups, like asthmatics. It contributes to acid rains.

4.3 Nitrogen Dioxide (NO2) – Nitrogen Dioxide is a brownish gas, easily detectable for its odor, very corrosive and highly oxidant. It is produced as the result of fossil fuels burning. Usually NO thrown to the atmosphere is converted in NO2 by chemical processes. In high concentrations, NO2 may lead to respiratory problems. Like SO2, it contributes to acid rains.

4.4 Air-Quality-Index: Function to convert the raw pollutant level received from each node to pollution standards called air quality index (AQI) using the formula.

AQI= (Pollution Level/Pollution Standard)*100

The pollution standard is defined according the air quality standards of a particular region. For example, the pollutant standard for CO, NO2, and SO2 are 20, 0.15, and 0.13 ppm, respectively. Following the air quality is divided into four categories. An index value of 0–100 corresponds to clean air, 101–125 represent light pollution, 126–150 signify four categories. An index value of 0–100 corresponds to clean air, 101–125 represent light pollution, 126–150 signify significant pollution, and above 150 means heavy pollution. In summary, the Air Quality-Index function returns a pollution category from the raw pollutant data.

5. Conclusion

A WSN Based Air Pollution Monitoring System was designed, implemented and tested using the wireless sensor network. The system is used to collect pollutant gases such as CO2, NO2, and SO2 from environment. The pollution data from various mobile sensor arrays is transmitted to a central several that make this data available to government authority. The data shows the pollutant levels and their conformance to local air quality standards. The system also uses the AQI to evaluate the level of health concern for a specific area. It also associates meaningful and very intuitive colors to the different categories, thus the state of air pollution can be communicated to the user very easily.(see table 2)

6. ACKNOWLEDGMENTS

The moment representing this project paper, we are grateful to all the respected professors for extending their valuable guidance to us. This was not just due to the efforts made by us but also the valuable guidance & facilities provided by our esteemed institution. Thus giving us an opportunity to amalgate our theoretical knowledge into presentation of project paper.with respect and deep gratitude we express our thanks to Prof. Pramod Ganjewar and Mrs. Uma Nagraj Computer Engineering (HOD) .We are thankful in particular to Prof. ShitalKumar Jain (Senior lecturer in Computer dept.) for his time to time guidance ,without which the completion of this project would have been impossible.

Our colleagues, who have been supportive throughout, are equally appreciable and deserving of our gratitude.

7. REFERENCES

[1]. N. Kularatna and B.H. Sudantha, "An environmental air pollution monitoring system based on the IEEE 1451 standard for low cost requirements," IEEE Sensors J., vol. 8, pp. 415–422, Apr. 2008.

[2]. Q. Cao, T. He, L. Fang, T. Abdelzaher, J. Stankovic, and S. Son, "Efficiency Centric Communication Model for Wireless Sensor Networks", in Proceedings of IEEE INFOCOM, pp. 1- 12, 2006.

[3]. Xu.N. "A Survey of Sensor Network Applications,"EEE Communications Magazine, Vol. 40, No.8, pp. 102-114, 2002.

[4]. Martinez, K., Hart, J. K., Ong, R., "Environmental Sensor Networks," IEEE Computer, Vol. 37, No. 8, pp. 50-56.

[5]. Nikheel A. Chourasia, Surekha P. Washimkar," ZigBee Based Wireless Air Pollution Monitoring" International Conference on Computing and Control Engineering (ICCCE 2012), 12 & 13 April, 2012

[6]. R. Rajagopalan and P.K. Varshney, "Data-Aggregation Techniques in Sensor Networks: A Survey," IEEE Communication Surveys and Tutorials, Vol. 8 (4), pp. 48-63, December 2006.

[7]. Mainwaring, A., Polastre, J., Szewczyk, R., Culler, D., Anderson, J. "Wireless Sensor Networks for Habitat Monitoring," ACM International Workshop on Wireless Sensor Networks and Applications, EUA.

[8]. F. Tsow, E Forzani, A. Rai, R. Wang, R. Tsui, S. Mastroianni, C. Knobbe, A. J. Gandolfi, and N. J. Tao, "A wearable and wireless sensor system for real-time monitoring of toxic environmental volatile organic compounds," IEEE Sensors J., vol. 9, pp. 1734–1740, Dec. 2009.

[9]. Y.J. Jung, Y.K. Lee, D.G. Lee, K.H. Ryu, and S. Nittel, "Air pollution monitoring system based on geosensor network," in Proc. IEEE Int. Geoscience Remote Sensing Symp., 2008, vol. 3, pp. 1370–1373.

[10]. W. Chung and C.H. Yang, "Remote monitoring system with wireless sensors module for room environment," Sens. Actuators B, vol. 113 no. 1, pp. 35–42, 2009

International Journal of Science and Engineering Applications (IJSEA)
Volume 2 Issue 4, 2013, ISSN - 2319-7560 (online)

Security Establishment in MANET Systems using FACES

P.Manivannan
Department of Information Technology
V.R.S. College of Engineering and Technology
Arasur, Villupuram Dt – 607107,
TN, India.

J.Shakila
Department of Information Technology
V.R.S. College of Engineering and Technology
Arasur, Villupuram Dt – 607107,
TN, India.

Abstract: Friend based Ad-hoc routing using Challenges to Establish Security (FACES) is an algorithm to provide secure routing in ad-hoc mobile networks. The scheme proposed has been drawn from a network of friends in real life scenarios. The algorithm is divided into four stages, viz. Challenge your neighbour, Rate Friends, Share Friends and Route through Friends. One of the major advantages of this scheme is that the nodes do not need to promiscuously listen to the traffic passing through their neighbours. The information about the malicious nodes is gathered effectively by using Challenges, which reduces the overhead on networks. As a result of this scheme of operation, the network is able to effectively isolate the malicious nodes which are left with no role to play in the ad-hoc network. One major benefit of this scheme is that the nodes do not need to promiscuously listen to the traffic passing through their neighbours. The information about the malicious nodes is gathered effectively by using Challenges. This reduces the overhead on the network significantly. Through extensive simulation analysis it was inferred that this scheme provides an efficient approach towards security and easier detection of malicious nodes in the mobile ad-hoc network.

Keywords: FACES, Challenges, Rate friends, Share Friends, Net Friends

1. INTRODUCTION

Wireless technologies have revolutionized the world of communications. It started with the use of radio receivers or transceivers for use in wireless telegraphy early on and now the term *wireless* is used to describe technologies such as the cellular networks and wireless broadband Internet. Although the wireless medium has limited spectrum along with a few other constraints as compared to the guided media, it provides he only means of *mobile communication*. Wireless ad-hoc networking is used for random and rapid deployment of a large number of nodes, which is a technology with a wide range of applications such as tactical communications, disaster relief operations, health care and temporary networking in areas that are not densely populated. A mobile ad-hoc network (MANET) [1] - [3] consists of mobile hosts equipped with wireless communication devices. The transmission of a mobile host is received by all hosts within its transmission range due to the broadcast nature of wireless communication and omni-directional antenna. If two wireless hosts are not within the transmission range in ad-hoc networks, other mobile hosts located between them can forward their messages, which effectively build connected networks among the mobile hosts in the deployed area.

1.1 Objective

In this paper, we present the design and propose an algorithm to establish secure routing in mobile ad-hoc networks. We name the algorithm as FACES which stands for Friend based Ad-hoc routing using Challenges to Establish Security. The name of the algorithm itself explanatory. We use trust establishment through friends and special challenges for authenticating the nodes. This provides a robust mechanism for thwarting attacks by isolating malicious nodes in the network. We also propose friend updating schemes and suggest a novel way to authenticate nodes using challenges, which is the basis of the algorithm. The algorithm tackles all the security challenges in an innovative way and gives a robust self-sustaining security mechanism without data is finally routed through the route with the greatest number of trusted friends. The quality of the route is determined by evaluating each and every node in the route and making a final decision about the quality of the route. To deal with eavesdropping we encrypt the data at the source using *public key cryptography*. A central authority such as a key distribution center can be very difficult to maintain in a mobile ad-hoc network. So, whenever a destination node receives a route request it sends its public key along with the route reply. The source uses that public key, which it receives from the most trusted route to encrypt the data that needs to be sent. In this way the chances of man in the middle attack are greatly reduced and eventually are eliminated as the friend circle becomes much more robust. The use of wireless ad-hoc networks also introduces additional security challenges that have to be dealt with. The weak links that cause these security challenges are as follows.

1.1.1 Easier to Tap

Since the media is nothing but air, it can be tapped easily.

1.1.2 Limited Capacity

The wireless medium has limited capacity and therefore requires more efficient schemes with less overhead.

1.1.3 Dynamic Nature

The self-forming, self-organization and self-healing algorithms required for ad-hoc networking, may be targeted to design sophisticated security attacks.

1.1.4 *Susceptibility to Attacks*

The wireless medium is more susceptible to jamming and other denial-of-service attacks. Attacks in MANETs can be broadly classified as: passive and active attacks. In passive attacks the intruder remains undetected and captures the data while the message is being transmitted over the network. Eavesdropping and traffic analysis mainly fall in this category. Unlike passive attacks, in active attacks the intruder/attacker can affect the communication by modifying the data, misleading the nodes in the network. As a matter of act various scenarios and threats can be developed based on these approaches.

2. RELATED WORK

This section discusses the previous work done in the field of secure routing in ad hoc networks. The goals of any secure routing protocol are to provide some or all of the properties such as Authentication, Access Control, Confidentiality, Privacy, Integrity, Authorization, Anonymity, Non-repudiation, Freshness, Availability, Resilience to attacks. Of these, Availability in particular targets denial of service (DoS) [5] attacks and has the ability to sustain the networking functionalities without any interruption due to security threats. The routing algorithms deal with the dynamic aspects of Mobile Ad-Hoc Networks in their own way depending upon the requirements of the system. Essentially a routing algorithm can behave in a reactive, proactive, or a combination of both, that is, in a hybrid way. Reactive algorithms are those that behave in an on-demand fashion, which means that these algorithms gather routing information in response to some event viz. start of a data session, route request messages, link failure messages etc. Proactive algorithms are those which gather essential information before hand, so that the information is readily available when an event occurs. Hybrid algorithms use both proactive and reactive components in order to try to combine the best of both schemes. The conventional routing protocols for MANETS are DSR [4] and AODV [6]. These conventional routing algorithms do not provide security and are prone to attacks caused by malicious nodes moving in the network. Since security is one of the major concerns of ad-hoc networks there is a need for secure routing schemes in ad-hoc networks. This can be achieved by using either of the following security based routing methods: payment-based systems, reputation-based systems and cryptography-based systems. All these systems have their own features. Of these, the reputation-based systems and the cryptography-based systems are the ones that are most widely used in ad-hoc networks. It has also been observed that most of the secure routing algorithms use cryptography as the central mechanism to implement security. Two of the most widely used algorithms for public key cryptography are RSA and Diffie – Hellman [7], [8]. A number of routing protocols [9] - [16] have been proposed towards providing security in ad-hoc networks. Some of the most widely discussed protocols are Authenticated Routing for Ad Hoc Networking (ARAN) [9], ARIADNE [10] and Watchdog Pathrater [11]. There have also been various secure routing techniques [14] - [16] that use multipath based routing where they break the data into different number of sub packets, encrypt them and then finally route them through different paths. In this work we have looked into the secure routing techniques DMR [14], TMR [15] and MTMR [16], and have designed the proposed FACES protocol to provide better security. These protocols [14] - [16] have been discussed in the following subsections, as these protocols are the ones that have been used for comparison with the proposed technique FACES.

2.1 Security Enhancement through Disjoint Multipath Transmission: DMR

DMR [14] provides a way to further secure the data transmitted along routes of a wireless ad hoc network after a potentially secure connection has been established between two nodes. In this method, the encryption/decryption key used is the message itself. The approach requires that the message is split into parts (sub-messages) and that the encrypted sub-messages be transmitted along different paths (routes) which are reception disjoint. The method partitions a 4n-bit message into two four n-bit parts called. Up to three redundant bits can be added in order to make the number of bits a multiple of four. Four encrypted n-bit parts, labeled are generated using the equations referred in [14]. For details regarding the encryption and decryption of the message, refer the technique discussed in [14]. This protocol takes advantage of the shortest path between the source and the destination. A modification of Dijkstra's algorithm is applied for this purpose. All nodes have positive weight. Every path that is returned and is a desired path automatically implies that a second path exists with the reception disjoint property. This set of paths will be used as the solution to the routing problem. Another feature used to determine the security of each selected route is the "priority" labeling. The nodes are labeled with a "priority" number according to the number of edges they are linked to. This indicates if a node can be trusted on sending a message with less chance of that message being grabbed by an adjacent node. In this method, the decryption of the original message requires all the encrypted parts. The security of this method lies in the fact that an enemy node or a corrupted node needs to intercept all the parts to be able to decipher the message. Failure to intercept one part gives no information about the original message.

2.2 Message Security using Trust-Based Multipath Routing : TMR

TMR [15] provides a method of message security using trust based multipath routing. In this approach, less trusted nodes are given lesser number of self-encrypted parts of a message, thereby making it difficult for malicious nodes to gain access to the minimum information required to break through the encryption strategy. Using trust levels, it makes multipath routing flexible enough to be usable in networks with "vital" nodes and absence of necessary redundancy. In addition, using trust levels, it avoids the non-trusted nodes in the routes that may use brute force attacks and may decrypt messages if enough parts of the message are available to them. This technique uses a variation of the trust models used in [17] and [18]. A node is assigned a discrete trust level in the range of to 4. A trust level of 4 defines a complete trust and a trust level of defines a complete distrust. These trust levels also define the maximum number of packets which can be routed

through those nodes. The trust level assigned to a node is a combination of direct interaction with its neighbors and the recommendations from its peers. A node assigns a direct trust level to its neighbor on the basis of acknowledgements received. The 4 n-bit message is divided into 4 n-bit parts, and encrypted using the equations referred in [15].The encrypted parts are then routed instead of the original message using multiple paths between the source and the destination nodes. These multiple paths between the source and the destination nodes are found using DSR. In this, the source node waits for a predefined time period in order to have multiple paths to the destination. The routing paths are finally selected from the set of obtained paths using a novel trust defined strategy in which a node with a trust level of is given at most parts of the packet to forward. This limits the possibility of a brute force decryption of the message. The routes are selected using a greedy approach on the basis of path length such that a node with a trust level of does not get more than packets on the route to the destination. At the destination, the message parts are then decrypted using the equations referred in [15].Thus, the TMR approach is found to be more secure than the multipath routing using disjoint paths (DMR), but it generally takes more time in route selection.

2.3 Message and Trust Based Multipath Routing: MTMR

MTMR [16] uses a trust assignment and updating strategy which can be used to identify and isolate malicious nodes without being hard on the resources of the network. It uses a parameter, the trust requirement of the message such that each message has a certain level of importance based on its content and type. This is the trust requirement of a particular message, which decides how the message will be routed. Therefore, only paths with certain trust level can be used for its forwarding. This further enhances the security of the system. Initially, each node is given a trust value of zero which indicates unknown trust level. Later this value may be incremented or decremented based on the behavior of the node. The trust levels have a range of values from for minimum trust and for maximum trust. Equations (1) and (2) are used for decrementing and incrementing the trust of a node. In these equations indicates the allowed number of misbehaviors that a node with a given value of trust can perform and, indicates the number of times a normal behavior was exhibited by a node with trust (1) & (2). If the trust is calculated as 1, then the value of will be equal to 2. Therefore, it will take two misbehaviors to reduce trust value to an immediate lesser trust level of 0. Similarly, for a node with trust level 4, eight (8) misbehaviors are allowed, also if a node with a current trust value as 3 has to rise to a trust level of 4, it will have to perform normally for at least 8 times. Equation (3) below (based on the technique referred in [19]) calculates the trust value of a given node by its neighboring nodes. In this equation, is the trust level that the node has of node is the trust level that node has observed on node , and represents the required trust level for the current message delivery.(3) The MTMR approach uses the message encryption inspired by cipher-block chaining (CBC) mode of block encryption referred in [20], [21]. It defines a trust based path selection strategy where a path with trust is given only parts of the packet to forward. This limits the possibility of brute-force decryption of the message by any node with lower trust value than the message. The multiple paths are calculated by DSR, by waiting for a specified period of time for the multiple *Route_Reply* packets to come from various paths. The paths are then arranged in an ascending order of hop-counts and descending order of trust levels. This step makes sure that the routes selected are of least hop-count besides being most trusted, so as to minimize the overheads and the path with highest trust is selected. Once the paths have been selected, the parts of the data packets are then transmitted through these selected paths based on the routing decisions discussed in [16]. Once the parts of the packets have been sent completely, the source then sends the hash of the complete packet as the final message. The hash message is calculated as a Cyclic Redundancy Check (CRC) variant [20].

3. FACES PROTOCOL

In this section, we discuss our proposed algorithm in detail. We start with the list of terms used in the protocol. This is followed by a detailed discussion of the algorithm and a list of security attacks thwarted by it.

3.1 List of Terms Used

3.1.1 Question Mark List

The list of nodes which are deemed suspicious by a particular node. This list is stored for each and every node in its data structure.

3.1.2 Unauthenticated List

The list of nodes of which no security information is present.

3.1.3 Friend List

This is the list of nodes which convey trust. Like the question mark list, a friend list is also stored for each node in its data structure. Friends are rated on a scale of 0 to 10.

3.1.4 Friend Request (FREQ)

This is a control packet which is used to initiate friend sharing. A node receiving this packet replies with the nodes in its friend list, unauthenticated list and the question mark list.

3.1.5 Data Rating (DR)

This is the rating given to nodes after they transmit some amount of data for the source node.

3.1.6 Friend Rating (FR)

This is the rating computed when nodes share their friend lists.

3.1.7 Net Rating (NR)

This rating is computed as a weighted mean of DR and FR.

3.1.8 Obtained Rating (OR)

The rating received during the friend sharing stage.

3.2 FACES Algorithm Description

Friend based Ad-hoc routing using Challenges to Establish Security (FACES) accomplishes establishment of friend networks in MANETs in the same way as in real life scenarios. We apply the same idea to develop the FACES algorithm. The proposed FACES algorithm is divided into the following four stages as shown in Figure 1(a) & 1(b) - *Challenge your neighbor, Rate Friends, Share Friends and Route through friends*.

The figure 1(b) also depicts the link/flow between the different stages of the algorithm. The routing of data in the protocol is on demand; that is whenever the need arises. But challenges, friend sharing and rating are periodic processes. This makes the FACES protocol a hybrid one. The *Challenge your neighbor* stage is designed to facilitate trust establishment for a new node in relation to the other nodes present in the network. *Rate Friends, Share Friends and Route through friends* gradually make the network robust in terms of the reliability of the nodes, and it is through these stages that the nodes gather data about each other and populate a *friend list* where the information about reliable nodes is kept. A node having its neighbors in its friend list does not need to challenge them before a data session. The idea of the FACES scheme is drawn from real life friend networks. When people meet in a new community or a group they are strangers to each other. Fig. 1(a) depicts a network of friends in a community. Tasks are completed by trusting one another unconditionally initially and with time the trust level increases with the number of successful task completions. Initially breach of trust is possible as no one has any information about the people with malicious intentions. However, with time, trust relationships are formed and we have a community where tasks are completed efficiently. The following sections discuss each of the stages in greater detail.

3.2.1 Challenge your neighbor

Challenge is a mechanism to authenticate nodes initially when no criterion is present. It is a basic test which a node has to complete in order to prove its honesty and integrity. Let us assume that the node challenges its neighbor node.

Step 1) When the network is newly initialized, each node is a stranger to another. Thus each node incorporates its neighbors in the *unauthenticated list*.

Step 2) The node picks one of the neighbors, and performs the usual *Share Friends Stage* (which will be discussed later).

Step 3) As a response the neighbor node either sends its friend list or the nodes from its *unauthenticated list* if the friend list is empty.

Step 4) On receiving the list, the node picks up a node which it can reach on its own and in the most efficient way. Let us say that this node is.

Step 5) Now the node has two ways to reach the node one through and another through a route already known to it.

Step 6) The node initiates a challenge and encrypts it with the public key of. It then sends it through both routes also includes its own public key with the challenge.

Step 7) The node sees the challenge as a normal data packet and routes it.

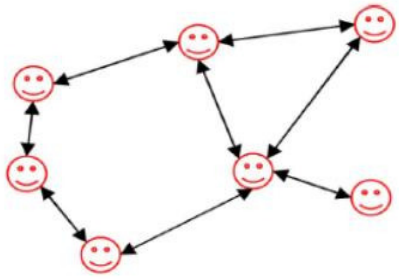

Figure.1(a) - Network of friends in a community

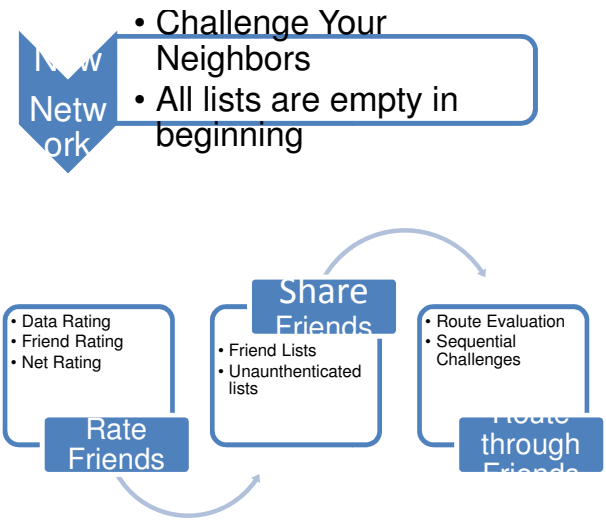

Figure.1(b) - FACES : Link / Flow between different stages

As decrypts the data packet and finds that it is a challenge it responds to the challenge. It then encrypts the response with public key that it obtained in STEP 6.

Step 8) Receives the result of the challenge from both routes and after decrypting, it compares them. If they are same then node adds node at the bottom of its friend list. In this way, node can authenticate node as a node which is behaving genuinely at least initially.

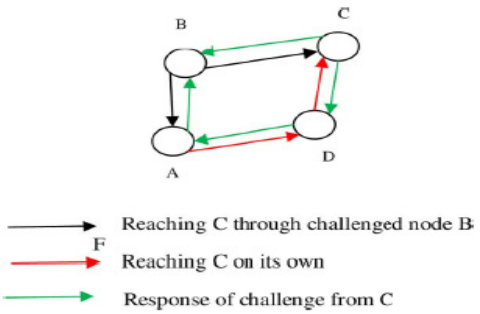

Fig. 2. Illustration of the Challenge.

Figure.2 gives an illustration of how the challenge is initiated by on disguised as a data packet for. The challenge is also routed through to Figure 2. Illustration of the challenge and the results obtained are compared to arrive at a decision about the node .However, there are some cases which might bring ambiguity in the mind of the reader. We discuss these cases though the method of questions. Each question is formulated to depict the working of this stage of the algorithm. Below, we provide the questions and the answers for the issues which test the suitability of the *Challenge Your Neighbor* Stage.

3.2.2 Description of the challenge

Each node is initialized with a pair of large prime integers which is secret to that node. When a node wants to send a challenge to a particular node it sends one of his random prime numbers to it and expects a response in return. The challenge process takes the following four steps for node challenging node.

Step 1) First it is initialized with

Step 2) When challenges, as described above. It sends a random prime number "n" as the challenge.

Step 3) computes *mod n* and sends the result to the two paths.

Step 4) compares the result from the two paths to arrive at a decision on as described above. Since and are all very large prime numbers it is impossible to determine and from the result of the *mod* function as that is known to be a hard problem. In this way, the nodes can authenticate each other through the challenge process. As the newly initialized nodes authenticate each other and a robust network of friends is formed, it becomes very difficult for a new malicious node to authenticate itself.

3.3 Rate Friends

Friends are rated on a scale of zero to ten. Initially each node has only those nodes in their friend list that completed the challenge successfully. Sharing of friend nodes is done in the *Share Friends* stage as the friend relation is transitive in nature that is a friend of friend includes in his friend list too. Each friend in the list has the following three classes of ratings: *Data Rating (DR)*, *Friend Rating (FR)* and *Net Rating (NR)*.

3.3.1 Data Rating

The data rating is updated by a node for its friend on the basis of amount of data it transfers for it. This is a significant metric for judging the quality of the node, as it portrays its battery power and general capacity to forward data packets. The DR of a friend node varies according to the number of data packets transferred through it. The net DR is calculated as a moving average of the last five data ratings. Equation (4) describes the moving average relation between a data rating and the previous five data ratings:(4) The DR for a particular session is calculated as (5) where is the number of data packets transmitted and is the factor by which we want the number of data packets to be related to the rating. The moving average is a significant tool to estimate the recent quality of node in terms of data forwarding. As and when a node drops data packets, we compute the negative value for one session of DR using as the number of data packets dropped. The exponential scaling on the number of data transferred is an effective tool to scale according the requirements of the network. We can change the value of according to the volume of data that is transferred trough the network. Keeping a value (of 1/100) ensures a smooth scaling from 1 to 10 for data packets up to 200 with a data rating of around 6 for 100 packets. As we increase the value of, the curve increases DR quickly towards the maximum value 10. As is decreased it smoothens the DR along the range of the data packets. Fig. 3 below shows the graph of DR versus the number of data packets transmitted up to 200 with.

3.3.2 Friend Rating

During the Friend Sharing stage a node asks for the friend list of node and incorporates the rating of friends in the following way.

1) If a node have common friend, then the node obtains the rating of the node from node as (6), shown at the bottom of the page. The idea behind this (6) is to incorporate the trust that node has on node while obtaining the rating of node from it. We further explain this through the use of two scenarios.

3.3.3 Net Rating

The idea behind calculating DR and FR is to have two opinions in front of each node. This is done because malicious nodes can identify some nodes for which they would work properly while for some they would drop packets. The DR acts as the soul opinion of the host node and FR acts as the opinion of its friend nodes. The Net Rating (NR) would be a weighted mean of the two ratings as given in equation (1):

$$NR = \frac{W_1 * DR + W_2 * FR}{W_1 + W_2} \quad \text{---------- (1)}$$

Where *W1* and *W2* would be the weights assigned to DR and FR respectively. The values of *W1*and *W2* are network dependent and can be learnt with experience.

4. SIMULATION RESULTS AND DISCUSSIONS

Figure.3 - Number of Hops

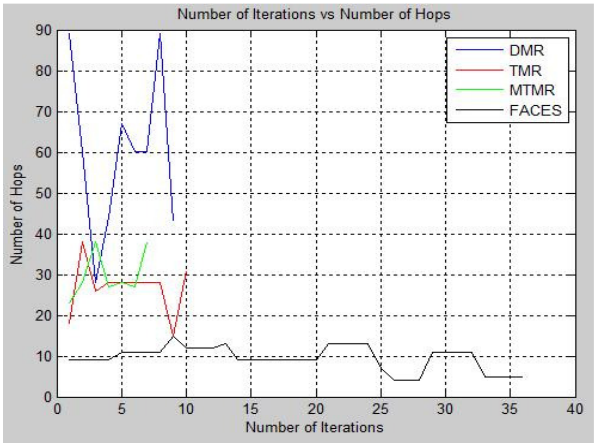

Figure.4 - Route Discovery

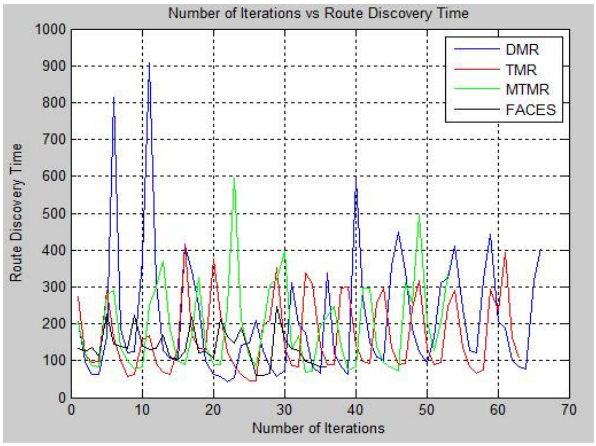

Figure.5 - Packet Loss

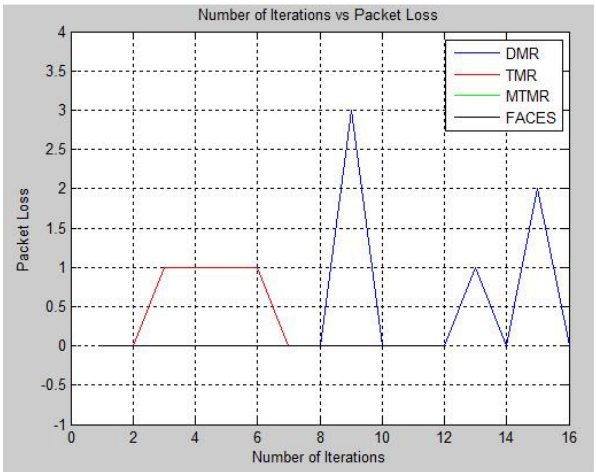

5. CONCLUSION AND FUTURE WORK

Mobile Ad-hoc network (MANETs) due to its dynamic nature has many challenges. Some of the major challenges are number of malicious nodes detected, number of hops, route discovery time, packet loss, energy and power consumption.

Many Routing algorithms namely DMR, TMR, MTMR and FACES have their own way in order to establish the trust and transmit packet securely. But Friend based protocol proved to be best in terms of number of malicious nodes detected, number of hops, route discovery time, packet loss, power consumption and energy.

After a logical analysis and extensive simulation of the FACES algorithm under different scenarios, we come to the conclusion that it offers robust scheme to afford security for mobile ad-hoc networks and performs better than the trust based protocols from which it was compared. Due to the absence of the need of promiscuous mode in the mobile nodes, the network has to bear a lot less overhead as compared to other secure routing schemes. The friends sharing scheme turns out to be an efficient mechanism to spread information about trusted nodes effectively in the system. In our protocol, we use challenges to authenticate any node compared to the other security protocols that use multipath routing and overhear the neighbor activities. To make a decision that a node is malicious, the multipath routing algorithms take much more time than FACES scheme which detects the malicious activity by checking the challenge reply. This on the other hand reduces overheads and hence reduces the chances of unsecured routing through faulty nodes. Due to these challenges, the FACES protocol works much better and provides more security than the other multipath routing protocols. In the future, we plan to implement existing secure routing protocols such as the ARIADNE and ARAN and compare them with the proposed FACES protocol. This would give a better picture about the standing of the FACES algorithm as compared to these long established secure routing protocols for MANETs.

6. REFERENCES

[1] D. P. Agrawal and Q.-A. Zeng, *Introduction to Wireless and Mobile Systems*. Pacific Grove, CA: Brooks/Cole, Thomson, 2002.

[2] I. Chlamtac, M. Conti, and J.-N. Liu, "Mobile ad-hoc networking: Imperatives and challenges," in *Ad-Hoc Networks*. New York: Elsevier, 2003, vol. 1, pp. 13–64, No. 1.

[3] L.Wang and N.-T. Zhang, "Locally forwarding management in ad-hoc networks," in *Proc. IEEE Int. Conf. Communications, Circuits and Systems and West Sino Expositions*, Jun./Jul. 2002, pp. 160–164.

[4] D. Johnson and D. Maltz, "Dynamic source routing in ad-hoc wireless networks," in *Book Chapter in Mobile Computing*, T. Imielinskiand H.Korth, Eds. Dordrecht, The Netherlands: Kluwer, 1996, pp. 131–181.

[5] A. Wood and J. A. Stankovic, "A taxonomy for denial-of-service attacks in wireless sensor networks," in *Handbook of Sensor Networks:*ll

[6] C. Perkins, E. Royer, and S. Das, Ad-Hoc on Demand Distance Vector (AODV) Routing Jul. 2003, Internet experimental RFC 3561.

[7] W. Diffie and M. E. Hellman, "New directions in cryptography," *IEEE Trans. Inform. Theory*, vol. IT-22, no. 6, pp. 644–654, 1976.

[8] M. S. Obaidat and N. Boudriga, *Security of e-Systems and Computer Networks*. Cambridge, U.K.: Cambridge Univ. Press, 2007.

[9] K. Sanzgiri, B. N. Levine, C. Shields, B. Dahill, and E. M. Belding-Royer, "A secure routing protocol for ad-hoc networks," in *Proc. 10thIEEE Int. Conf. Network Protocols (ICNP)*, Paris, France, Nov. 12–15,2002, pp. 78–89.

[10] Y. Hu, A. Perrig, and D. B. Johnson, "Ariadne: A secure on-demand routing protocol for ad-hoc networks, "*WirelessNetw.*, vol. 11, no. 1–2, pp. 21–38, Jan. 2005.

[11] S. Marti, T. J. Giuli, K. Lai, and M. Baker, "Mitigating routing misbehavior in mobile ad hoc networks," in *Proc. MobiCom 2000*, Boston, MA, Aug. 2000, pp. 255–265.

[12] M. G. Zapata and N. Asokan, "Securing ad-hoc routing protocols," in *WiSe'02: Proc. of 1st ACM Workshop on Wireless Security*, Atlanta, GA, Sep. 28, 2002, pp. 1–10.

[13] P. Papadimitratos and Z. J. Haas, "Secure link state routing for mobile ad-hoc networks," in *IEEE International Symposium on Applications and the Internet-Workshop on Security and Assurance in Ad-Hoc Networks*, Orlando, FL, Jan. 2003, p. 379.

[14] T.Haniotakis, S. Tragoudas, and C. Kalapodas, "Security enhancement through multiple path transmission in ad-hoc networks," in *2004 IEEE Int. Conf. Communications*, Jun. 2004, vol. 7, pp. 4187–4191.

[15] P. Narula, S. K. Dhurandher, S. Misra, and I. Woungang, "Security in mobile ad-hoc networks using soft encryption and trust based multipath routing," *Sci. Direct Comput. Commun.*, vol. 31, pp. 760–769, 2008.

[16] S. K. Dhurandher and V. Mehra, "Multi-path and message trust-based secure routing in ad-hoc networks," in *Proc. Int. Conf. Advances in Computing, Control and Telecommunication Technologies (ACT 2009)*, Trivandrum, India, Dec. 28–29, 2009, pp. 189–194.

[17] A. Abdul-Rahman and S. Hailes, "A distributed trust model," in *Proc. 1997Workshop on New Security Paradigms*, Langdale, Cumbria, U.K., Sept. 23–26, 1997, pp. 48–60, NSPW'97. ACM Press, New York.

[18] A. A. Pirzada, A. Datta, and C. McDonald, "Propagating trust in ad-hoc networks for reliable routing," in *Proc. 2004 Int. Workshop on Wireless Ad-Hoc Networks*, May–Jun. 2004, pp. 58–62.

[19] Z. Liu, A. W. Joy, and R. A. Thompson, "A dynamic trust model for mobile ad-hoc networks," in *Proc. 10th IEEE Int. Workshop on Future Trends of Distributed Computing Systems*, May 2004, pp. 80–85.

[20] W. Stalling, "Cryptography and network security, principles and practice," in *Book Chapter in Block Ciphers and Data Encryption Standard*, 3rd ed. Upper Saddle River, NJ: Prentice-Hall, 2006, pp. 62–94.

[21] M. S. Obaidat and N. Boudriga, *Security of e-Systems and Computer Networks*. Cambridge, U.K.: Cambridge Univ. Press, 2007.

[22] P. J. Rousseeuw and C. Croux, "Alternatives to the median absolute deviation," *J. Amer. Statist. Assoc.*, vol. 88, no. 424, pp. 1273–1283, Dec. 1993.

International Journal of Science and Engineering Applications
Volume 2 Issue 4, 2013, ISSN – 2319-7560 (online)

Multi-Touch Gesture Application Using QT for Linux/Windows Operating System

Arnav Sonara
Computer Department
MIT AOE, Alandi(d)
Pune, India

Ajinath Funde
Computer Department
MIT AOE, Alandi(d)
Pune, India

Sumit Jadhav
Computer Department
MIT AOE, Alandi(d)
Pune, India

Swapneel Lodha
Computer Department
MIT AOE, Alandi(d)
Pune, India

Om Shankar
Computer Department
MIT AOE, Alandi (d)
Pune, India

Abstract: Now a days, user interaction considers time as its primary factor. Using menu bar, tool bar for accessing the actions to be performed take much time. So, the main purpose of this paper is to demonstrate how to minimize the access time of various features of the application by multi touch. It makes user interaction much easier by accessing various features using multi touch gestures. We are introducing idea for gesture support on applications like Image Viewer, Document Viewer, etc. We are making use of *Pan, Pinch, Swipe, and Rotate…etc.* gestures to make user interaction easier and faster. This idea can be implemented using C++ Qt Framework, developed by Nokia as it has great support for GUI and Gesture programming. The main advantage of Qt is that it is cross platform, once coded, it can be deployed on various operating systems.

Keywords: Input devices and strategies, Touchpad, Multi-touch, Gestures, widgets, Computer Access

1. INTRODUCTION

1.1 Motivation

THIS PAPER IS MOTIVATED BY TWO PRIMARY CONCERNS, THE NEED FOR BETTER DESKTOP COMPUTER ACCESS, PARTICULARLY FOR LINUX/WINDOWS OPERATING SYSTEM AND SECOND IS PLATFORM INDEPENDENT. TO REDUCE THE EXCESSIVE USE OF MOUSE & CURSOR METHOD OR KEYBOARD IS THE MAIN GOAL OF THIS PROJECT.

1.2 Need of Multi-touch

Accessing to computer and information technology is increasing dramatically in present scenario. So, time is the primary factor to access these resources. Accessing these features using mouse and cursor method takes much time. As in present scenario, there is great revolution in touchpad, they are able to detect up to ten fingers and we can make use of this feature to implement various gestures which can be then further used in various applications to trigger some action to be performed.

1.3 Why C++ Qt Framework?

Qt has great support for GUI and Gesture programming. Also it is cross platform application framework and makes use of standard C++. It has inbuilt tools like *"Meta Object Compiler"*and *"qmake"*. "*Meta Object Compiler"* is used for automatic code generation and "*qmake"* is used for compiling project on different platform without changing the code. It has vast number of predefined classes which can be used for various purposes during development of applications. The "*QObject*" is the root class of all other classes of Qt and which is mandatory for "*SIGNAL-SLOT*" functionality to work properly. It also contain UIC compiler which is used to convert ".ui" file generated by Qt Designer into C++ header file. It contains *Qt Assistant* which provides documentation for various predefined classes and functions already defined in Qt. So while implementing idea presented in this paper we can easily make use of this documentation and thus more user friendly than any other framework.

1.4 How Qt Supports Gesture Programming?

For events, Qt has library called *"QEvent"*. There is one function *"eventFilter()"* function in "*QAbstractEventDispatcher"*class that is used to detect whether the particular input is an event or not. For gesture events *enum* is defined in *"QEvent"* class as *"QEvent::Gesture"* and various other events like keyboard event, mouse event, etc. If no event is recognized then index returned by *"eventFilter()"*function is NONE if any gesture is recognized it returns index 198. After recognizing gesture events it uses "*QGestureRecognizer*"class which inherits *"QEvent"* class and *"QGesture"* class.For implementing various gesture it has predefined different gesture class for implementing operation on application.Various gesture supporting classes are "*QswipeGesture*", "*QPanGesture"*, "*QTapGesture","QTapAndHoldGesture*", etc. These gesture classes have many different functions,data,static data and static functions. For implementing custom gesture it is mandatory to use *"QTouchEvent"* class. It contain function like "*start ( )"*, "*update ( )", "delete ( )",* etc. to implement custom gesture.

Fig. 1 Gesture Types gives brief idea about how these gestures are to be performed on touchpad.

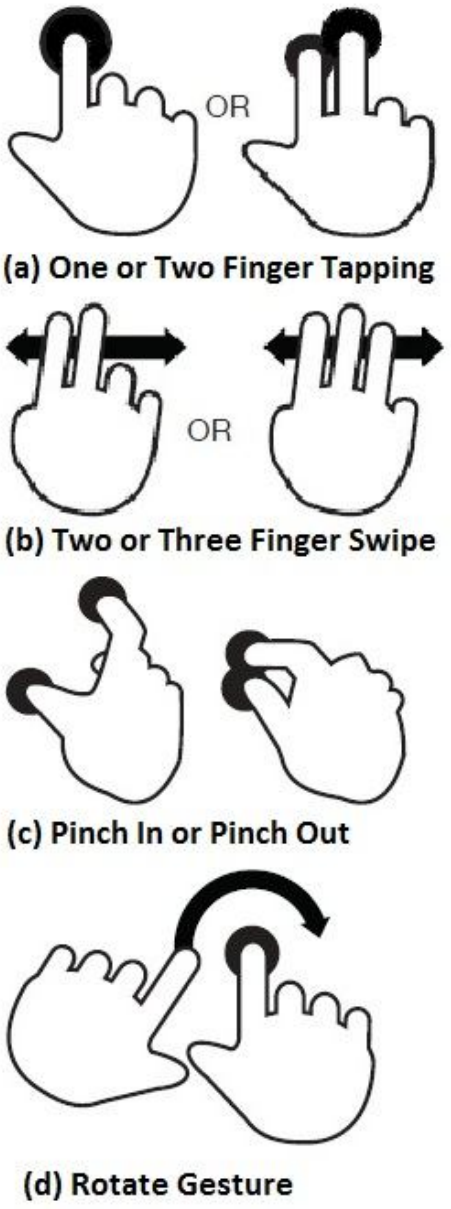

Fig. 1 Gesture Types

2. CURRENT WORK IN THIS AREA

Presently, many touchpad applications are developed but they are not supported in different operating system platform. Synaptic developed these features for windows operating system. But these softwares are not supported by other operating system Symbian and Linux. So, the platform dependency is the main problem of these softwares.

Also, for Linux operating systems (Ubuntu/Fedora), only edge-scrolling & two finger scrolling are available by default. In addition to it, two finger scrolling does not work in many flavours of Linux. Two/three finger tapping, two/three finger swipe, pan gesture are still not available in various flavours of Linux. Human Computer Interaction software company's engineers are working in this area to make these gestures available for different operating system.

3. MULTI-TOUCH SOFTWARE ARCHITECTURE

Although the platform and application may be different, the basic architecture of the Multi-touch software remains same. It consists of several different layers as shown in figure among viz. Input Hardware Layer, Hardware Abstraction Layer, Transformation Layer, Interpretation Layer, Widget Layer.

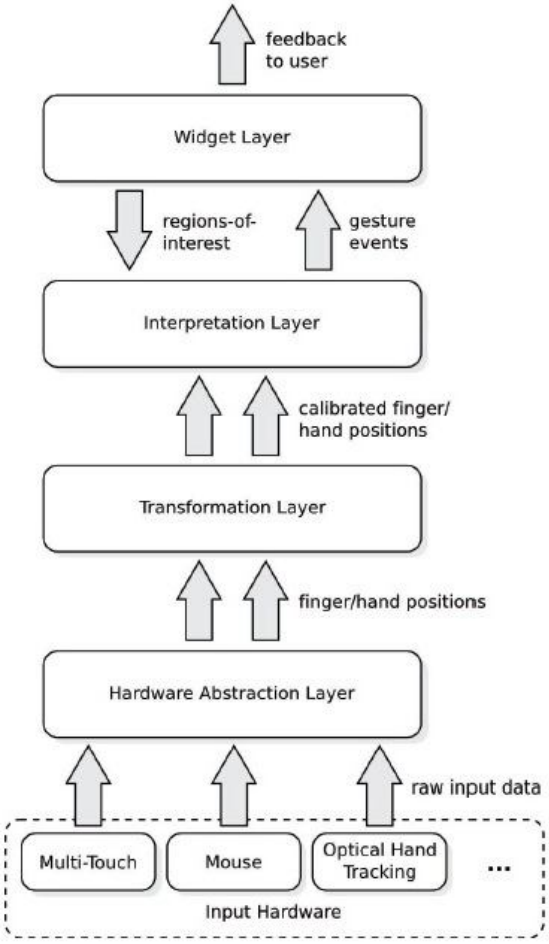

Fig. 2 MULTI-TOUCH SOFTWARE ARCHITECTURE

The *Input Hardware Layer* is the lowest layer. It generates raw tracking data in the form of electrical field measurement.

This information is then passed to *Hardware Abstraction Layer* which processes it to detect position of fingers, hands and/or objects from the raw data as per the capabilities of input device. This newly generated information is then sent to the *Transformation Layer*.

Transformation Layer converts absolute co-ordinate of device into relative co-ordinates of screen. At this stage, data provided by the touchpad is ready for interpretation.

The main task of *Interpretation Layer* is to assign some meaning to the movement of fingers performed on touchpad, i.e. gesture, using knowledge about regions on the screen. A region is a polygonal area, given in screen coordinates in which a certain set of events will be matched. Regions can be seen as a generalization of the window concept which is used in all common GUIs. For each region, a list of gestures to match is maintained. When the correct events occur within a region, the corresponding gesture is triggered and passed to the next layer.

As the mapping from motion to meaning can be expected to change for different input devices, a capability description has to be supplied which provides this mapping. This final part of our framework is the *widget layer*. Its task is to register and update regions of interest with the interpretation layer and then act on recognized gestures by generating visible output.

4. HIGH LEVEL DIAGRAM

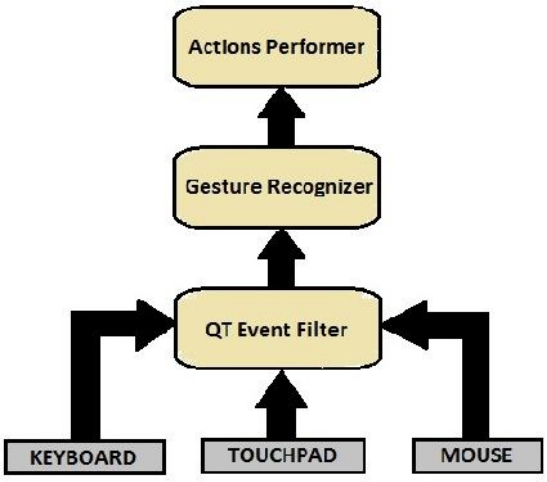

Fig. 3 Interaction of Input Devices with Application

5. WORKING AND IMPLEMENTATION

While implementing idea given in this paper first of all the image viewer's main window will be opened. The main window of this application is actually the custom *Qt Designer Class* which inherits *QMainWindow*class. *QMainWindow*has much functionality predefined in it, which are generally required by main window like *Menu Bar, Tool Bar, Status Bar, etc.* To add items in *menu bar* and *tool bar*, use of Qt Designer is the easiest way. We can also write actions, add icons, add tool tip and shortcuts for *menu bar* items using *Action Editor* of *Qt Designer*.

From *menu bar*, we have to select "Open…" option to load particular directory containing some image files. For this purpose, *QDir* and *QFile* classes are more than sufficient. From these image files, any one of the image will get displayed on the screen. Next, Previous, Zoom In, Zoom Out, Rotate, etc. these actions can be performed on the current image from *menu bar* or *tool bar*. But the main objective of this paper is to perform all these actions by making some gestures on Touchpad.

To do this, first of all, we have to enable gestures on *QLabel* object which we are using for displaying the image by passing appropriate argument to describe gesture type. This can be done by calling "*grabGesture ()"* function inside the constructor of image viewer.

e.g.

```
grabGesture(Qt::PanGesture);
grabGesture(Qt::PinchGesture);
grabGesture(Qt::SwipeGesture);
```

On generation of particular gesture, "*eventFilter()"* function will be called to detect whether it is gesture event or any other input event. If gesture event is detected then it will call "*GestureRecognizer"* to know which type of gesture is performed on current image. "*Gesture Recognizer"* class will perform the task of gesture filtering in which, it will detect which type of gesture is performed by the user and it will call the appropriate method of "*Action Performer"* class. Finally, "*Action Performer"* will contain implementations of various actions to be performed by the application such as Next, Previous, Zoom, Rotate, etc.

Now, in order to zoom the image, we don't need to drag the cursor to *menu bar->View->Zoom In or tool bar->Zoom* and then Click on it. What we just have to do is, perform the Pinch Gesture and it will automatically zoom the image, which is clearly time saving as compared to previous method.

6. FUTURE SCOPE

We have presented this paper for touch pad with support only for two/three fingers detection. But now we are planning to work with touchpad having multi touch support up to ten fingers. Due to this greatest advantage, we will be able to implement numerous custom gestures which involve up to ten fingers and maximum of the laptop functionality can be accessed only by using touchpad and gestures very speedily.

After this, we have planned to integrate multi touch gesture support in open source operating systems like Linux by working with windows session management, so that one can access the whole laptop just by using touchpad and gestures.

7. CONCLUSION

We have demonstrated the use of multi-touch gestures in accessing the laptop computers and also showed that this is the most time efficient way to access various features of different applications using image viewer application.

8. ACKNOWLEDGEMENT

We would like to express our sincere gratitude for the assistance and support of a number of people who helped us.

We are thankful to **Ms. Kavitha S.,** Department of Computer Engineering, MIT AOE, our internal guide for her valuable guidance that she provided us at various stages throughout the project work. She has been a source of motivation enabling us to give our best efforts in this project.

We are also grateful to **Prof. Uma Nagaraj,** Head of Computer Department, MIT AOE and other staff members for encouraging us and rendering all possible help, assistance and facilities.

We are also thankful to **Mr.Amar More**, Project Coordinator of Computer Department of MIT AOE for appreciating us to use Qt as our framework for implementing this paper.

9. REFERENCES

[1] JasminBlanchette, Mark Summerfield, "C++ GUI Programming with Qt 4, Second Edition"

[2] Johan Thelin, "Foundations of Qt Development"

[3] Daniel Molkentin, "The Book of Qt 4The Art of Building Qt Applications"

[4] Florian Echtler and Gudrun Klinker, "A Multitouch Software Architecture." Technische Universität München Institutfür Informatik Boltzmannstr. 3D-85747 Garching, Germany {echtler,klinker}@in.tum.de

[5] Hao Lu and Yang Li, "Gesture Coder: A Tool for Programming Multi-Touch Gestures by Demonstration." Google Research 1600 Amphitheatre Parkway Mountain View, CA 94043 yangli@acm.org

[6] Gilles Bailly, Jörg Müller and Eric Lecolinet, "Design and Evaluation of Finger-Count Interaction:Combining multitouch gestures and menus." 1Quality and Usability Lab, Telekom Innovation Laboratories, TU Berlin, Germany 2Telecom ParisTech, CNRS LTCI UMR 5141, France.

International Journal of Science and Engineering Applications (IJSEA)
Volume 2 Issue 4,2013, ISSN-2319-7560 (Online)

Building Software Architecture using Architectural Design Patterns

U.V.R. Sarma
Department of CSE
CVR College of Engg.
Ibrahimpatan(M),
R.R. District, A.P., India

Neelakantam Pavani
Department of IT
CVR College of Engg.
Ibrahimpatnam(M)
R.R. District, A.P., India

P. Premchand
Osmania University,
Department of CSE,
Hyderabad, A.P., India

Abstract: this paper discusses how Software Architectural design patterns could be used to build the architecture of a system. The application of design patterns helps to improve the quality of software architecture and to reduce the flaws in the architecture. Generic architectural design patterns for real-time software components are customized to suit the functionality of system. This is illustrated using the Solar TErrestrial RElations Observatory (STEREO) a case study based on NASA's STEREO mission. The customized design patterns are validated using IBM Rational Rhapsody. These validated design patterns form templates for further use in building the architecture of flight software.

Keywords: Software Architectural Design Patterns, UML 2.0, IBM Rational Rhapsody Developer for Java, Flight Software, Components.

1. INTRODUCTION

This paper customizes generic design patterns to suit the functionality of Solar Terrestrial Relations Observatory (STEREO). The Design Patterns are built and also validated using IBM Rational Rhapsody. The variability in the design patterns can also be represented in the diagrams by using Product Line UML based Software Engineering methodology by Gomaa [1] to enable the use of design patterns for any other systems in DRE domain.

The STEREO case study is chosen as the number of flight software anomalies are increasing in number and also as they lead to major losses [2]. Thus as per the functionality of STEREO ten generic design patterns are identified and are customized to suit the functionality of STEREO. The functionality of each component of STEREO is depicted by using state charts. The paper uses the IBM Rational Rhapsody developer for Java 7.6.1 to build the design patterns and also to build and validate the state charts. Validating the design patterns and state charts will better describe the functionality of each component of the system and will check the design patterns for their functional correctness.

2. TOOL SUPPORT : IBM RATIONAL RHAPSODY

This paper uses a tool called IBM Rational Rhapsody Developer for Java 7.6.1 to build and execute the state machines [3]. The generic design patterns are customized and validated using the tool. The functionality of the components in the design patterns can be depicted in Rational Rhapsody by using the Rhapsody's Action language which is similar to java and Event handling infrastructure.

IBM Rational Rhapsody's action language can be used to capture actions and to execute the model. This action language can be used to make the diagrams executable by representing the actions each object performs and also the messages the objects pass to other objects when an event occurs. The message passing can be represented in state charts, by depicting the message passing and the respective transitions. The action language is similar to Java, except there are a few additional reserved words. For example, GEN is a reserved word used to generate asynchronous messages as events. The messages must be specified on the consumer's provided interface in order to be invoked.

Ex: PClass1.gen(new msg());

Where PClass1 is the *provided interface* which also specifies the port through which the message is sent and msg() method that is called to implement the appropriate task. Code for these methods can be written using the action language. When an event is generated, IBM Rational Rhapsody event handling infrastructure handles the routing of events from the producer to the consumer. When the consumer component receives the event, the appropriate state transition is taken and actions within that state are performed. Thus, executable state charts represent the functional behavior of the components of the system. However the coding required for IBM Rational Rhapsody differs by the Object eXtended Framework (OXF) involved which depends on the Developer Edition (Java or C++). That is the action language semantics and syntax differs based on the OXF.

IBM Rational Rhapsody is an excellent tool to create dynamic UML diagrams using Real-time UML that is UML 2.0. These executable state charts and Object Model Diagrams can be validated using Rational Rhapsody. Rhapsody is also used to generate code for the diagrams.

3. UML 2.0 AS ARCHITECTURAL DESCRIPTION LANGUAGE (ADL)

The Unified Modeling Language (UML 1.0) [4] was first introduced as a formal graphical language to represent the system as static diagrams but was later revised to represent the functionality of components of real-time systems as UML 2.0 also called as Real-Time UML.

Architecture Description Language (ADL) is defined as "a language (graphical, textual, or both) for describing a software system in terms of its architectural elements and the relationship among them" [4]. UML is widely accepted language by practitioners. This paper uses UML 2.0 to represent the components of the systems in terms of an Object Model diagram and state chart diagrams. The UML 2.0

diagrams are represented using the Component and Connector views (C&C views, for short) [5]. They present architecture in terms of elements that have a runtime presence (e.g., processes, clients, and data stores) and pathways of interaction (e.g., communication links and protocols, information flows, and access to shared resources). *Components* are the principal units of run-time interaction or data storage. C*onnectors* are the interaction mechanisms among components. The UML extensibility mechanisms (i.e., stereotypes, tagged values, constraints) are used to interpret the functionality of the system in the diagrams [6].

In UML 2.0, the components are created as Composite classes and each of the components should have ports to interact with the external environment. Each port again requires an interface for it to interact. The interfaces are of two types *Provided Interface* and *Required Interface.* Two components with ports and their interfaces can be linked for communication. The ports and their interfaces should be compatible, that is one component having a *required interface* (depicted as semi circle) can interact with only a component that provides the interface (depicted as full circle).

4. SOLAR TERRESTRIAL RELATIONS OBSERVATORY (STEREO)

The STEREO mission is a two year mission from NASA with a goal to provide the first ever three dimensional images of the Sun by studying the nature of Coronal Mass Ejections (CME). The mission involves using two nearly identical three-axis stabilized spacecraft in heliocentric orbit, which is an orbit around the sun. Since the spacecraft is far away from Earth, the STEREO FSW relies less on real-time ground commanding and more on autonomous functionality. Additionally, since STEREO operates in a heliocentric orbit it requires guidance and control algorithms along with propulsion hardware to achieve and maintain its orbit.

The STEREO spacecraft contains four payload instrument packages to accomplish its scientific mission. The payload packages are In-situ Measurements of Particles And CME Transients (IMPACT), PLAsma and SupraThermal Ion Composition (PLASTIC), STEREO/WAVES (S/WAVES), and Sun Earth Connection Coronal and Heliospheric Investigation (SECCHI). The IMPACT package measures solar wind electrons, energetic electrons, protons, heavier ions, and the in situ magnetic field strength and direction. PLASTIC measures the composition of heavy ions in the ambient plasma, protons, and alpha particles. S/WAVES measures the generation and evolution of traveling radio disturbances. Finally, SECCHI uses remote sensing imagers and coronagraphs to track CMEs.

The payload instruments collect data 24 hours a day, even when the spacecraft is in communication with the ground. During events of interest, the FSW must also enable the appropriate instruments to collect data at higher sampling rates. The FSW is responsible for performing some processing on the data such as data compression and formatting the data into telemetry packets. Additionally, the FSW must collect and store data from all the payload packages. The data is pushed from the instrument data buffers to the FSW during predetermined time intervals and using predefined data rates.

STEREO maintains its orientation in space using a three-axis stabilization technique, as opposed to a spin stabilization technique. In STEREO's three-axis stabilization technique, reaction wheel assemblies (RWAs) are mounted on various sides of the spacecraft and the appropriate RWAs are fired to make slight changes to the spacecraft's orientation. To adjust the spacecraft's attitude, adjustments are managed by firing thrusters to push STEREO to the proper attitude. Attitude determination and control is managed autonomously onboard the spacecraft by the FSW. The FSW determines the attitude and orientation using measurements from one star tracker, six sun sensors, and one Inertial Reference Unit (IRU). If the FSW determines that the attitude and orientation are out of the acceptable range, then it must determine and send the appropriate commands to the RWAs and/or thrusters to adjust the spacecraft's attitude.

STEREO uses two movable solar array appendages to generate power. The FSW is responsible for positioning the solar arrays toward the sun. Onboard power is controlled using a Power Distribution Unit (PDU). To maintain a consistent temperature, STEREO spacecraft uses both active and passive means of thermal control. The active measurers include thermistors and electric heaters to ensure the spacecraft remains a consistent temperature throughout the spacecraft since one side of the STEREO is facing the Sun and the other does not. The FSW is responsible for monitoring the spacecraft temperatures and sending commands to the appropriate heaters to adjust the temperature. STEREO downlinks its data once per day to the ground through NASA's Deep Space Network (DSN) station in Canberra, Australia. To communicate with the ground, STEREO contains a Low Gain Antenna (LGA), Medium Gain Antenna (MGA), and High Gain Antenna (HGA) that will be used depending on where the spacecraft is in orbit. The FSW is responsible to selecting and using the right antenna at the right time. The LGA and MGA are fixed, however the STEREO FSW is responsible for autonomously controlling the HGA so that is pointed at Earth.

Based on the functionality of STEREO ten design patterns have been identified to depict the functionality of STEREO. The design patterns identified are listed in the table 1.

Table 1. STEREO Design Patterns

Feature	Design Pattern
High Volume Command Execution	**STEREO Hierarchical Control Design Pattern**
High Volume Telemetry Storage and Retrieval	**STEREO Compound Commit Design Pattern**
High Volume Telemetry Formation	**STEREO Pipes and Filters Design Pattern**
Quick Check	**STEREO Sanity Check**
Event Driven Payload Data Collection	**STEREO Payload data Client Server Design Pattern**
Ground Driven Housekeeping Data Collection	**STEREO Housekeeping data Multiple Client Multiple Server Design Pattern**
Event Driven Housekeeping Data Collection	**STEREO Housekeeping data Client Server Design Pattern**
Housekeeping Data Checks	**STEREO Housekeeping Checks Multicast**
Spacecraft Clock	**STEREO Spacecraft Clock Multicast**
Memory storage Device fault Detection	**STEREO Memory Storage Device Watchdog.**

The reason for selecting the above Design patterns is described below:

4.1. Hierarchical Control Design Pattern:

STEREO FSW must interact with ten components to implement its functionality. Hierarchical controller would be appropriate to implement such functionality where a separate controller is identified for components implementing similar actions. Example a Payload subsystem controller is identified to control the behavior of the four payload devices of STEREO. Thus a hierarchical control design pattern best suites the working of STEREO.

4.2. Compound Commit:

The data collected from different instruments of STEREO is to be stored or retrieved in a "all-or-nothing" methodology. That is either all the telemetry data is to be stored or nothing is to be stored by the components, similarly for retrieval of telemetry data.

4.3. Pipes and Filters Design Pattern.

The transformation of information into telemetry packets is done by Pipes and Filters Design Pattern. It increases throughput capacity of the system by adding multiple homogeneous (identical) channels.

4.4 Sanity Check

The Sanity Check design pattern is a pattern to improve reliability and ensure that the system performs more or less as expected. If a problem is detected, then the system is put into a failsafe state, which is a state that is always known to be safe. This design pattern is included because it provides a level of reliability to the Pipes and Filter design pattern. This design pattern is suitable to use on DRE applications that have reliability requirements but do not have high availability requirements.

4.5 Payload Data Multiple Client Multiple Server Pattern

The STEREO spacecraft contains four payload instrument packages to accomplish its scientific mission. The payload packages are In-situ Measurements of Particles And CME Transients (IMPACT), PLAsma and SupraThermal Ion Composition (PLASTIC), STEREO/WAVES (S/WAVES), and Sun Earth Connection Coronal and Heliospheric Investigation (SECCHI). The IMPACT package measures solar wind electrons, energetic electrons, protons, heavier ions, and the in situ magnetic field strength and direction. PLASTIC measures the composition of heavy ions in the ambient plasma, protons, and alpha particles. S/WAVES measures the generation and evolution of traveling radio disturbances. Finally, SECCHI uses remote sensing imagers and coronagraphs to track CMEs. A separate client and server for each of the payload instruments are created to collect the information whenever the controller signals to collect.

4.6. Housekeeping Multiple Client Multiple Server Design Pattern

The health of the satellite is maintained by collecting the information of the health or working of each of the component. This information is sent to the ground station. The ground station checks this information and sends any signals if necessary to check and modify the components. The collection of housekeeping information is done by this Design Pattern. Again a separate client and server component is created for ten components of STEREO.

4.7. Housekeeping Data Client-Server Design Pattern

This design pattern is used to represent the collection of housekeeping data from the client when an event occurs. When a request for a particular housekeeping data occurs in the form of an external event, this design pattern collects the information.

4.8. Housekeeping Data Checks Multicast

The housekeeping data checks design pattern performs certain checks on the housekeeping data at regular intervals and multicasts the messages to various components.

4.9. Spacecraft Clock Multicast Design Pattern

This pattern is used to send time signals to the Controller and input and output components of the system.

4.10. Memory Storage Device Watchdog Design Pattern

The memory storage device in STEREO is EEPROM. The Memory Storage Watchdog Design Pattern is selected to check the working of the memory storage device that is the EEPROM at regular intervals.

These ten design patterns are implemented in IBM Rational Rhapsody.

5. IMPLEMENTATION

Two design patterns are explained based on the functionality of STEREO. The UML diagrams built and validated using IBM Rational Rhapsody.

5.1 STEREO Hierarchical Control Design Pattern

The Hierarchical Control Design Pattern is selected as the components in STEREO cannot be controlled by a Centralized Controller. Also STEREO being away from the Earth, most of the processing needs to be done in the satellite itself. So different subsystems have been identified and each

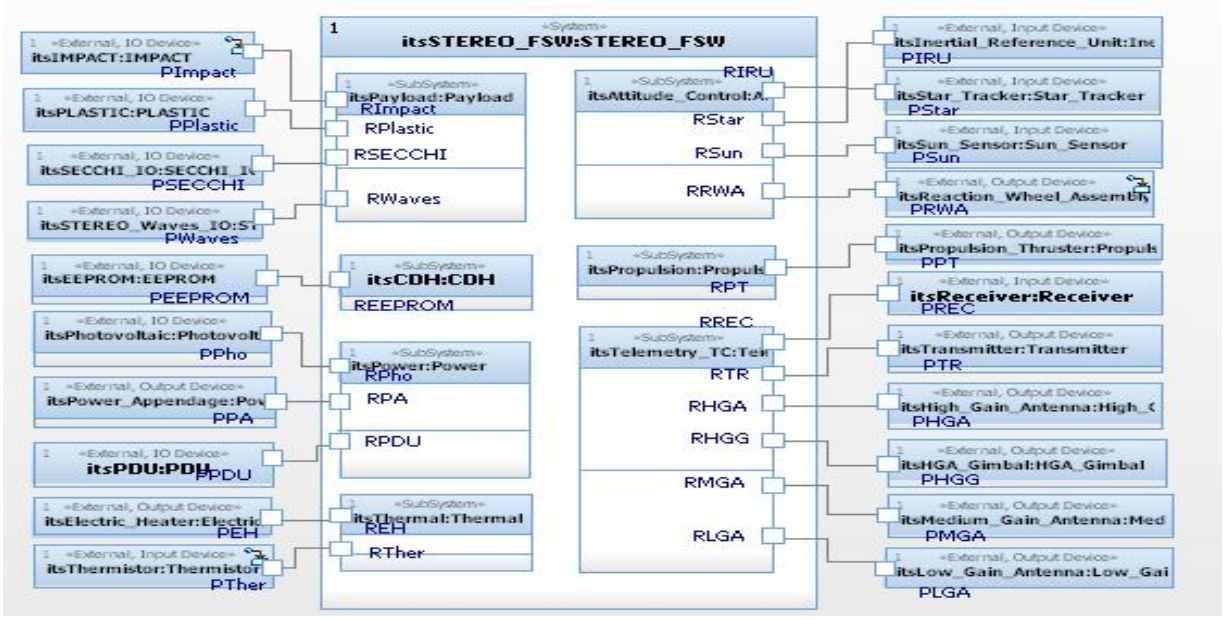

Figure 1 Object Model Diagram for Hierarchical Controller

of the subsystem takes care of the working of the components under it. This is depicted in the Object Model Diagram of the Hierarchical Control Design pattern Figure 1.

Each of the components is interconnected to their respective subsystems by the use of ports. IBM Rational Rhapsody is an excellent tool to represent the components of the system and their interconnections using the Component and Connector view of UML 2.0. The ports act as the interface to enable the component to interact with the external world. Each of the ports realizes interfaces which can be Provided interface or Required interface, which are not shown in the diagram for readability. The interfaces should be specified as part of the contract feature of the port.

The stereotypes may be used to identify the components as Input, Output or IO Component. Next a state chart diagram is built for each of the components as shown below figure 2, figure 3 and figure 4.

Next, the executable version of the design pattern involves potentially adding application specific states, actions, and activities to the state machines based on the application's features. For example, if the application features refine some behavior, then this can be modeled as sub-states. Also, if the component must send a message to an application specific variant or if application specific logic is required then this is modeled as an action or activity within a state or transition.

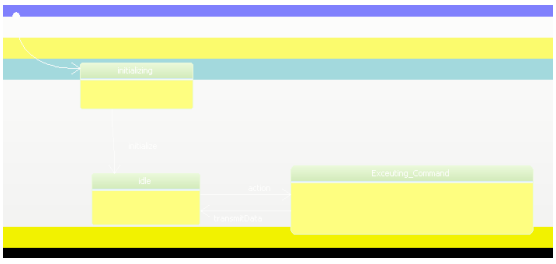

Figure 2 State chart diagram for Output component

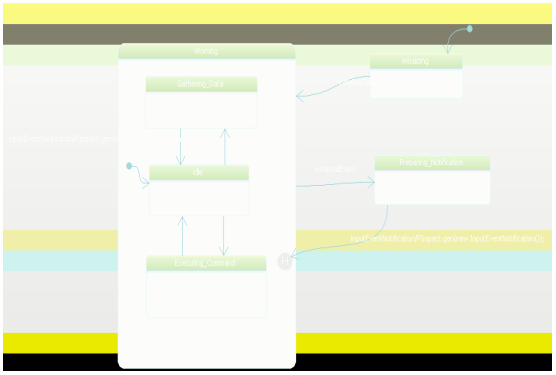

Figure 3 State chart diagram for IO Component

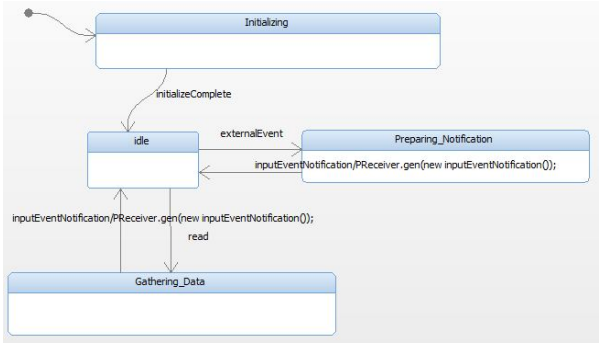

Figure 4 State Machine for Star_Tracker_IC

5.2 Memory Storage Watchdog Design Pattern

The Watchdog design pattern (Douglass 2003) is a lightweight design pattern to improve system reliability by making sure the processing is going as expected. This design pattern is included because it provides a lightweight approach to providing reliability. This pattern ensures the reliable working of the memory storage device that is EEPROM.

When the process is going as expected, the Watchdog receives stroking messages from the component it is monitoring. If it does not receive a stroking message within a given amount of time, the watchdog assumes a fault has occurred and sends out an alarm.

The FSW Memory Storage Device Watchdog Executable Design Pattern contains the components necessary to monitor the memory storage device for faults. The components and their behavior are common at the FSW and thus there are no SNOE specific customizations to this design pattern.

A *watchdog,* used in common computing parlance, is a component that watches out over processing of another component. In SNOE Watchdog is used to check the memory storage device for faults. Its job is to make sure that nothing is *obviously* wrong, just as a real watchdog protects the entrance to the henhouse without bothering to check if in fact the chickens inside are plotting nefarious deeds. The watchdog ensures that the memory storage device works properly. It checks the device and its functionality in predefined intervals.

The simplicity of the Watchdog Pattern is apparent from Figure 5. The *Actuator Channel* operates pretty much independently of the watchdog, sending a *liveness* message everyso often to the watchdog. This is called *stroking* the watchdog. The watchdog uses the timeliness of the stroking to determine whether a fault has occurred.

- ***Actuation Channel***

This is the channel that contains components that perform the end-to-end actuation required by the system. "End-to-end" means that it includes the sensing of control signals from environmental sensors, sequential or parallel data processing, and output actuation signals. It contains no components in common with the *Watchdog.*

- ***Actuation Data Source***

The *Actuation Data Source* is the source of sensed data used for control of actuation.

- ***Actuator***

The *Actuator* actor is the actual device performing the actuation.

- ***Data Transformation***

As in the other patterns, these components process the sensing data in a sequential fashion to compute the ultimate actuation output. This can be done with a single datum running all the way through the channel before another is acquired or with multiple data in various stages of processing simultaneously to provide a serial or parallel *Actuation Channel,* respectively.

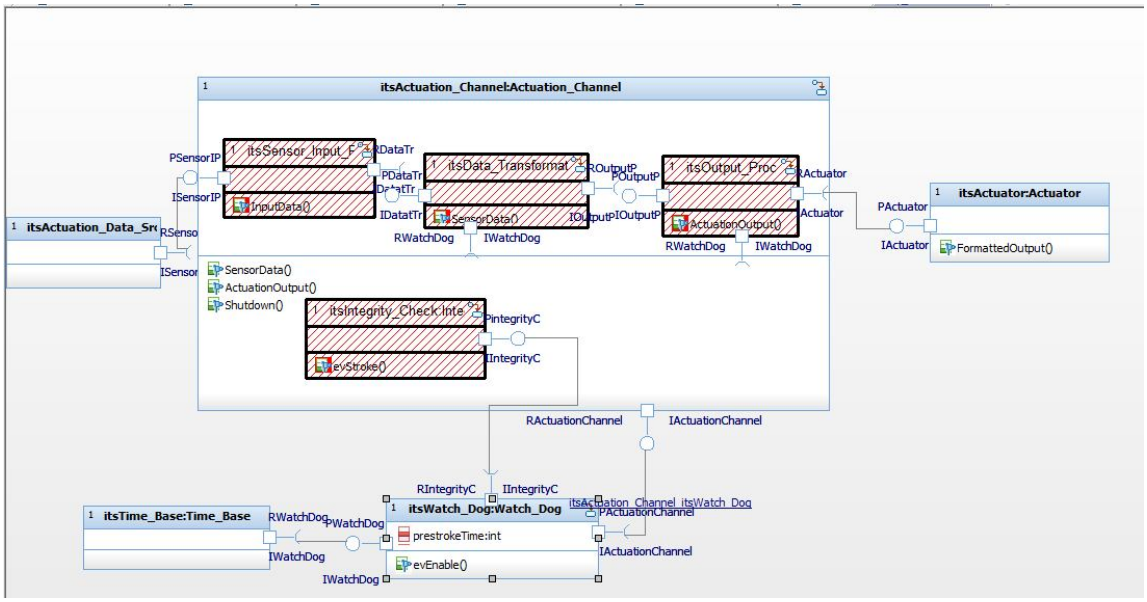

Figure 5 Object Model Diagram of Watchdog Design Pattern

- ***Sensor Input Processing***

The *Sensor Input Processing* component is a device driver for the *Actuation Data Source* actor. It performs any initial formatting or transformations necessary for the particular *Actuation Data Source* sensor.

- ***Integrity Checks***

This component is (optionally) invoked on every valid stroke of the *Watchdog.* This can be used to run a periodic Built In Test (BIT), check for stack overflow of the tasks, and so on**.**

- ***Output Processing***

This is a device driver for the *Actuator* actor. It performs any final formatting for transformations necessary for the particular *Actuator.*

- ***Timebase***

The *Timebase* is an independent timing source (such as an electronic circuit) used to drive the *Watchdog.*

- ***Watchdog***

The *Watchdog* waits for a stroke event sent to it by the components of the *Actuation Channel.* If the stroke does occur within the appropriate timeframe, the *Watchdog* may command integrity checks to be performed. If it does not, then it shuts down the *Actuation Channel.*

Some watchdogs check that the stroke comes neither too quickly nor too slowly. The statechart for such a time-range watchdog is shown in Figure 6. For some systems, protection against a timebase fault is safety-critical. In such cases, it is preferable to have an independent timebase. This is normally a timing circuit separate and independent from the one used to drive the CPU executing the *Actuation Channel.*

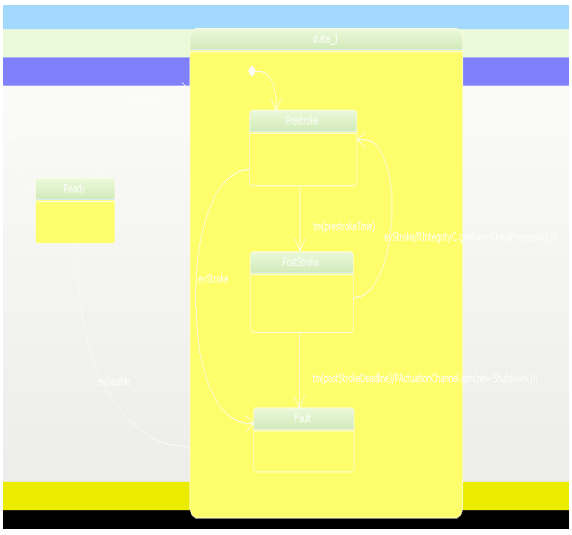

Figure 6 State machine for Watchdog

As mentioned before, if the watchdog is to provide protection from timebase faults, a separate electronic circuit *must* supply an independent measure of the flow of time. This means an independent timing circuit, usually driven by a crystal, but the timebase may be driven by an R-C circuit. Note, however, that the watchdog detects a *mismatch* between the two timing sources.

When the watchdog is stroked, it is common to invoke a BIT (Built In Test) of some kind to ensure the proper execution of other aspects of the system. These actions can either return a Boolean value indicating their success or failure, or may directly cause the system to shut down in the case of their failure. For example, the watchdog may execute an action on the evStroke transition (see Figure 6) that checks for stack overflow and performs CRC checks on the executing application software. If it does a similar check on the application data, it must lock the data resources during this computation, which can adversely affect performance.

When watchdog fires because it hasn't been stroked within the specified timeframe, it invokes some safety measure, normally either shutting down the system or causing the system to reset.

Similarly, the *Object Model Diagrams* and *state machines* for all the identified design patterns are developed and validated.

6. RESULTS

This paper validates the design patterns using the tool IBM Rational Rhapsody. Rational Rhapsody generates the code for the design patterns and validates the design patterns using 'build' option. Thus the functionality of design patterns can be verified during the design phase and thus reduce the number of anomalies in flight software. This validation of design patterns for functional correctness was not possible in static UML diagrams using UML 1.0. Rational Rhapsody also enables the animation of statecharts by generating events to check the behavior of the component. The figure 7 is an example of animated statechart of client component where the bright colored state indicates the present state of the component after the requestNeeded event is generated. Events can be generated manually while executing the state charts and thus transitions between the states can be checked. There by ensuring about the functionality of the components.

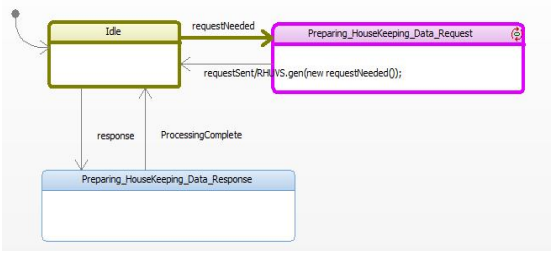

Figure 7. Animated State Chart for Client

Thus the functionality of every component in the design pattern can be validated to build an error free Architecture.

7. CONCLUSIONS

This paper uses generic architectural design patterns in the DRE domain to build the architecture of a satellite. The design patterns are customized to suit the functionality of the satellite and are also validated to reduce the risk of errors occurring after implementation. Also the design patterns are made executable to be used in the future for any other DRE domain.

8. FUTURE ENHANCEMENTS

This paper can be extended by including the performance validation. Also various other options of Rhapsody can be used to better represent the functionality and performance of design patterns.

9. REFERENCES

[1] H. Gomaa. 2005. *Designing Software Product Lines with UML: From Use Cases to Pattern-Based Software Architectures,* Addison-Wesley Object Technology Series.

[2] Julie Street Fant, Hassan Gomaa, Robert G. Pettit. 2011. *Architectural Design Patterns for Flight Software*, 14th IEEE International Symposium on Object/Component/Service-Oriented Real-Time Distributed Computing Workshops.

[3] D. Harel. 1997. Executable object modeling with statecharts, 18th International Conference on Software Engineering.

[4] B.Bharathi, Dr.D.Sridharan. 2009. *UML as an Architecture Description Language,* International Journal of Recent Trends in Engineering.

[5] Software Architecture Description & UML Workshop, Hosted at the 7th International Conference on UML Modeling Languages and Applications <<UML>> 2004, October 11-15, 2004, Lisbon, Portugal.

[6] Clements. P. 2002. et.al.: *Documenting Software Architectures, Views and Beyond*, Addison-Wesley, Boston, MA, USA.

International Journal of Science and Engineering Applications
Volume 2 Issue 4, 2013, ISSN-2319-7560 (Online)

Facial Feature Extraction Based on Local Color and Texture for Face Recognition using Neural Network

S.Cynthia Christabel
Sethu Institute of Technology.
Kariapatti.

M.Annalakshmi
Sethu Institute of Technology.
Kariapatti.

Mr.D.Prince Winston
SSCE
Aruppukottai.

Abstract: For the purpose of face recognition (FR), the new color local texture features, i.e., color local Gabor wavelets (CLGWs) and color local binary pattern (CLBP), are being proposed. The proposed color local texture features are able to exploit the discriminative information derived from spatiochromatic texture patterns of different spectral channels within a certain local face region. Furthermore, in order to maximize a complementary effect taken by using color and texture information, the opponent color texture features that capture the texture patterns of spatial interactions between spectral channels are also incorporated into the generation of CLGW and CLBP. In addition, to perform the final classification, multiple color local texture features (each corresponding to the associated color band) are combined within a feature-level fusion framework using Neural Network. Particularly, compared with gray scale texture features, the proposed color local texture features are able to provide excellent recognition rates for face images taken under severe variation in illumination, as well as some variations in face images.

Keywords: Color face image identification, Gabor Transform, LBP, DWT, GRNN.

1. INTRODUCTION

In pattern recognition and computer vision due to the wide range of applications includes video surveillance, biometric identification, and face indexing in multimedia contents. As in any classification task, feature extraction is of great importance. Recently, local texture features have gained reputation as powerful face descriptors because they are believed to be more robust to variations of facial pose, expression, occlusion, etc. In particular, Gabor wavelets and local binary pattern (LBP) texture features have proven to be highly discriminative for FR due to different levels of locality. There has been a limited but increasing amount of work on the color aspects of textured image analysis. Results in these works indicate that color information can play a complementary role in texture analysis and classification/recognition, and consequently, it can be used to enhance classification/recognition performance. In the paper "Classification with color and texture: Jointly or separately", an empirical evaluation study is performed which compares color indexing, gray scale texture, and color texture methods for classification tasks on texture images data set taken under either constant (static) or varying illumination conditions. Experimental result shows that, for the case of static illumination condition, color texture descriptors generally perform better than their gray scale counterparts. In the paper "Experiments in color texture analysis", three gray scale texture techniques including local linear transform, Gabor filtering, and co-occurrence methods are extended to color images. The paper reports that the use of color information can improve classification performance obtained using only gray scale texture analysis techniques.

In the paper "Perceptually uniform color spaces for color texture analysis: An empirical evaluation", incorporating color into a texture analysis can be beneficial for classification /recognition schemes. In particular, the results showed that perceptually uniform color spaces and Hue, Saturation, and Value (HSV) perform better than Red, Green, and Blue (RGB) for color texture analysis. Following the aforementioned studies, it is natural to expect better FR performance by combining color and texture information than by using only color or texture information. However, at the moment, how to effectively make use of both color and texture information for the purpose of FR still remains an open problem. The objective of this paper is to suggest a new color FR framework, which effectively combines color and texture information, aiming to improve FR performance. The main contributions of the paper are:

1) This paper proposes the first so-called color local texture features. Specifically, the development of two effective color local texture features, i.e., color local Gabor wavelets (CLGWs) and color LBP (CLBP), both of which are able to encode the discriminative features derived from spatiochromatic texture patterns of different spectral channels (or bands) within a certain local region. In addition, to make full use of both color and texture information, the opponent color texture features that capture the texture patterns of spatial interactions between spectral bands are incorporated into the generation of CLGW and CLBP. This allows for acquiring more discriminative color local texture features, as compared with conventional gray scale texture features, for improving FR performance.

2) The effective way of combining color local texture features has not been explored in the current FR works. This paper suggests the feature-level fusion approach in order to integrate multiple color local texture features [each extracted from an associated color component (or spectral) image] for the final classification using Neural Network.

2. EXISTING RELATED WORK

There are two main applications where extraction of facial features can play an important role. They are Gender Classification and Face Recognition.

Face Recognition Methods

Face recognition is one of the biometric methods of identifying individuals on the basis of prior knowledge about facial features and structure. Face recognition draws attention as a complex task due to noticeable changes produced on appearance by illumination, facial expression, size, orientation and other external factors. The paper deals with various techniques and methodologies used for resolving the problem .We discuss about appearance based, feature based, model based and hybrid methods for face identification. Conventional techniques such as Principal Component Analysis (PCA), Linear Discriminant Analysis (LDA), Independent Component Analysis (ICA), feature based Elastic Bunch Graph Matching (EBGM) and 2D and 3D face models are well-known for face detection and recognition.

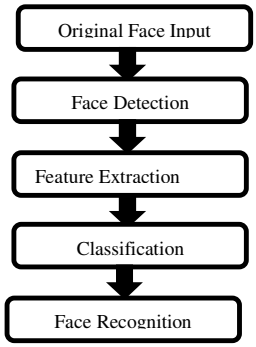

Fig 1. Feature Extraction Applications

Introduction to Face Recognition System

Face detection and recognition has emerged as an active area of research in fields such as security system, videoconferencing and identification. As security deserves prime concern in today's networked world, face recognition can be used as a preliminary step of personal identity verification, facial expression extraction, gender classification, advanced human and computer interaction. It is a form of biometric method utilizing unique physical or behavioral characteristics.

Face recognition is considered to be a complex task due to enormous changes produced on face by illumination, facial expression, size, orientation, accessories on face and aging effects. The difficulty level increases when two persons have similar faces.
Usually, face recognition systems accomplish the task through face detection, facial feature extraction and face recognition.

Face Recognition –Different Approaches

Generally, face identification technique can be considered as image based or feature based. The image based methods uses predefined standard face patterns whereas feature based techniques concentrate on extracted features such as distance between eyes, skin color, eye socket depth etc. More specifically, face recognition techniques fall in three categories, holistic, feature based model based and hybrid approaches.

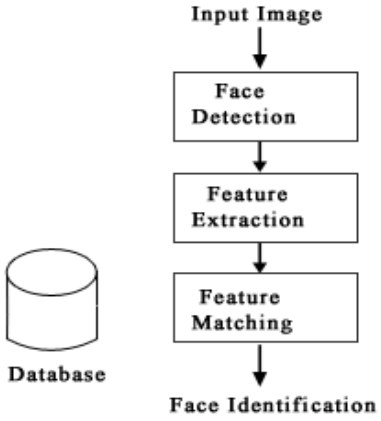

Fig 2. Face Recognition System

Holistic Approach

In holistic or appearance based approach, the whole face region is considered as the input data to the face recognition system. Examples are Eigen faces, fisher faces, probabilistic Eigen face etc. These techniques help to lower the dimensions of the dataset without tampering the key characteristics. Principal Component Analysis (PCA), Linear Discriminant Analysis (LDA), and Independent Component Analysis (ICA) are the most widely used holistic methods.

Feature Based Approach

The heart of any feature based algorithm is the localization and extraction of features on the face. Dynamic link structure and Hidden Markov Model methods belong to this category.

Hybrid Approach

Human perception system recognizes faces using local facial features and the whole face region information. The hybrid method is more akin to human perception system since it is influenced by both feature based and holistic methods. This approach is most effective and efficient in the presence of irrelevant data. The key factors affecting performance depend on the selected features and the techniques used to combine them.
Feature based and holistic methods are not devoid of drawbacks. Feature based method is sometimes badly affected by accuracy problem since accurate feature localization is its very significant step. On the other hand, holistic approach uses more complex algorithms demanding longer training time and storage requirements.

3. PROPOSED WORK

The proposed color FR system model using color local texture features consists of three major steps: color space conversion and partition, feature extraction, and combination and classification. A face image represented in the color space is first translated, rotated, and rescaled to a fixed template, yielding the corresponding aligned face image. Subsequently, the aligned color image is converted into an image represented in another color space. Note that not only conventional linear or nonlinear color spaces (e.g.YC_bC_r, or L*a*b*) but also new color spaces devised for the purpose of FR can be used for color space conversion. Each of the color-component images of current color model is then partitioned into local regions.

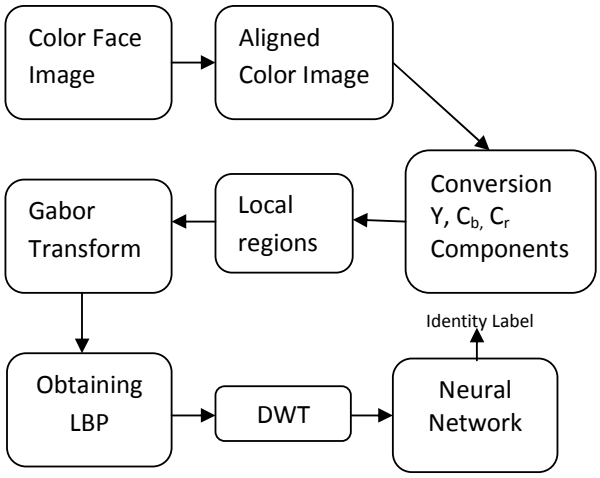

Fig.3. Proposed color gender classification system model based on color local texture features.

In the next step, texture feature extraction is independently and separately performed on each of these local regions. Since texture features are extracted from the *local* face regions obtained from different *color channels*, they are referred to as "color local texture features." Note that the key to FR using color information is to extract the so-called *opponent* texture features between each pair of two spectral images, as well as unichrome (or channel wise) texture features. This allows for obtaining much more complementary texture features for improving the FR performance, as compared with grey scale texture feature extraction, where only the luminance of an image is taken into account.

Since color local texture features (each obtained from the associated local region and spectral channel) are available, we have to combine them to reach the final classification. To this end, multimodal fusion techniques are employed for integrating multiple color local texture features for improving the FR performance.

GABOR FEATURE

Gabor Faces

Gabor filters, which exhibit desirable characteristics of spatial locality and orientation selectively and are optimally localized in the space and frequency domains, have been extensively and successfully used in face recognition. The Gabor kernels used are defined as follows:

Where and define μ & υ the orientation and scale of the Gabor kernels, respectively=(x, y), and the wave vector is defined as,

The Gabor kernels are all self-similar since they can be generated from one filter, the mother wavelet, by scaling and rotating via the wave vector. Hence, a band of Gabor filters is generated by a set of various scales and rotations. In this paper, we use Gabor kernels at five scales and eight orientations with the parameter to derive the Gabor representation by convolving face images with corresponding Gabor kernels. For every image pixel we have totally 40 Gabor magnitude and phase coefficients, respectively, that is to say, we can obtain 40 Gabor magnitude and 40 Gabor phase faces from a single input face image.

The Local Binary Pattern (LBP)

The local binary pattern operator is defined as a grey-scale invariant texture measure, derived from a general definition of texture in a local neighborhood. Through its recent extensions, the LBP operator has been made into a really powerful measure of image texture, showing excellent results in many empirical studies. The LBP operator can be seen as a unifying approach to the traditionally divergent statistical and structural models of texture analysis. Perhaps the most important property of the LBP operator in real-world applications is its invariance against monotonic grey level changes. Another equally important is its computational simplicity, which makes it possible to analyze images in challenging real-time settings. The LBP method and its variants have already been used in a large number of applications all over the world.

Gabor Volume Based LBP on Three Orthogonal Planes (GV-LBP-TOP)

LBP is introduced as a powerful local descriptor for micro features of images. The basic LBP operator labels the pixels of an image by thresholding the 3 3-neighborhood of each pixel with the center value and considering the result as a binary number (or called LBP codes). Recently, the combination of Gabor and LBP has been demonstrated to be an effective way for face recognition.

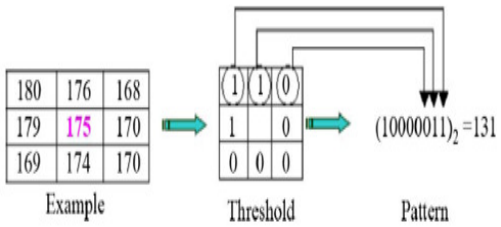

Fig.4. Basic LBP operator

This proposes to explore discriminative information by modeling the neighboring relationship not only in spatial domain, but also among different frequency and orientation properties. Particularly, for a face image, the derived Gabor faces are assembled by the order of different scales and orientations to form a third-order volume, where the three axes X, Y, T denote the different rows, columns of face image and different types of Gabor filters, respectively.

It can be seen that the existing methods essentially applied LBP or LXP operator on XY plane. It is natural and possible to conduct the similar analysis on XT and YT planes to explore more sufficient and discriminative information for face representation. GV-LBP-TOP is originated from this idea.

It first applies LBP analysis on the three orthogonal planes (XY, XT, and YT) of Gabor face volume and then combines the description codes together to represent faces. Fig. 3 illustrates examples of Gabor magnitude and phase faces and their corresponding GV-LBP codes on XY, XT, and YT planes. It is clear to see that the codes from three planes are different and, hence, may supply complementary information helpful for face recognition. After that, three

histograms corresponding to GV-LBP-XY, GV-LBP-XT, and GV-LBP-YT Codes are computed as

$$Hj(i) = \sum I(fj(x,y) = l), l = 0,1,.,.,L_j - 1$$

in which is an indication function of a Boolean condition and expresses the GV-LBP codes in th plane (: XY; 1: XT; 2: YT), and is the number of the GV-LBP code.

The GV-LBP-TOP histogram is finally derived by concatenating these three histograms to represent the face that incorporates the spatial information and the co-occurrence statistics in Gabor frequency and orientation domains and, thus, is more effective for face representation and recognition.

Effective GV-LBP

The aforementioned GV-LBP-TOP is of high computational complexity. The Length of the histogram feature vector and the computational cost are threefold compared to those of LGBPHS, so it is not very efficient in practical application. To address this problem, this paper proposes an effective formulation of GV-LBP (E-GV-LBP) which encodes the information in spatial, frequency and orientation domains simultaneously and reduces the computational cost. For the central point, and are the orientation neighboring pixels; and are the scale neighboring ones; and are the neighboring pixels in spatial domains. Like in LBP, all the values of these pixels surrounded are compared to the value of the central pixel, threshold into 0 or 1 and transformed into a value between 0and 255 to form the E-GV-LBP value.

$$E - GV - LBP = \sum_{p=0}^{7} 2^p S\,(Ip - Ic)$$

The E-GV-LBP codes based upon 40 Gabor magnitudes and phase faces for an input face image. The histogram features are then computed based upon the E-GV-LBP codes to provide a more reliable description as

$$H(i) = \sum_{x,y} I(f(x,y) = i), l = 0,2,.,.,L - 1$$

Where I (.) □ {0, 1} is an indication function of a Boolean condition and f (.) denotes the E-GV-LBP codes, and L is the number of the E-GV-LBP codes.

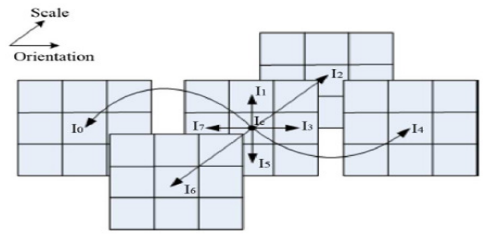

Fig 5. Formulation of E-GV-LBP.

NEURAL NETWORK CLASSIFIER

For each image the DWT analysis is performed on the LBP of the obtained features and the wavelet coefficients (five level decomposition is performed) are normalized, then it is trained using General Regression Neural Networks (GRNN). GRNN is one of the type neural networks that can be used for prediction. In this work GRNN is used to predict the in between training data values
n the last page should be as close to equal length as possible.

4. RESULTS & DISCUSSION

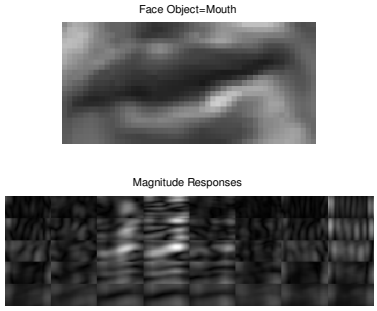

Fig.6. Magnitude Responses of Face Object – Mouth

This figure shows the magnitude responses of Face Object – Mouth under the feature extraction of the color local Gabor wavelets.

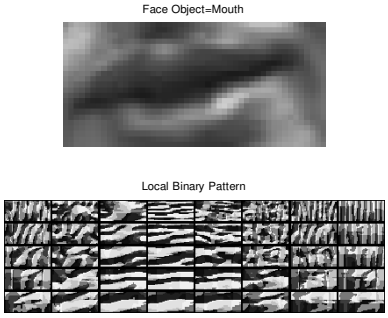

Fig.7. Local Binary Pattern of Face Object – Mouth

This figure shows the local binary pattern of Face Object - Mouth under the feature extraction of the color LBP.

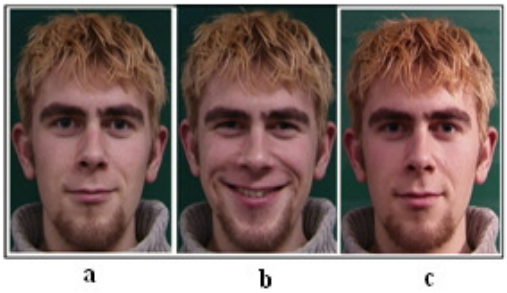

Fig.8.a. Sample Image in the training database, Fig.8.b. Sample Expression Variation Image in the test database, Fig.8.c. Sample Illumination Variation Image in the test database

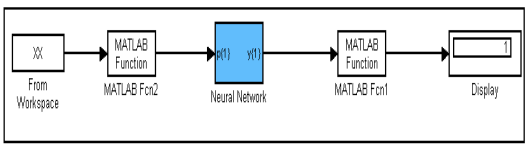

Fig.9. MATLAB Simulink diagram of the Neural Network Classifier

5. CONCLUSION

This work has investigated the contribution of color to existing texture features for improving the FR performance. Also how to effectively exploit the discriminating information by combining color and texture information, as well as its fusion approach has been examined. Color FR methods based on CLBP and CLGW significantly outperform the methods relying only on texture or color information. Color local texture features allows for a significant improvement in low-resolution face images, as compared with their gray scale counterparts. The final classification is performed using the DWT based Neural Network. The study in this work has been limited to evaluating the effectiveness of color local texture features that are extracted from fixed color-component configuration consisting of three components (such as RQCr). Hence, for the future work, the method of selecting an optimal subset of color components (from a number of different color spaces), aiming to obtain more discriminating color local texture features for FR can be developed.

6. REFERENCES

[1] Jae Young Choi, Yong Man Ro,(2012) 'Color Local Texture Features for Color Face Recognition IEEE Transactions On Image Processing', Vol. 21, No. 3, pp . 1366 -1380.

[2] Bowyer K. W. (2004) 'Face recognition technology: Security versus privacy' IEEE Technol. Soc. Mag Vol. 23 No. 1 pp. 9–19

[3] Jain A. K., Ross A. and Prabhaker S. (2004) 'An introduction to biometric recognition' IEEE Trans. Circuits Syst. Video Technol Vol. 14 No. 1 pp. 4–20

[4] Choi J. Y., De Neve W., Ro Y. M. and Plataniotis K. N. (2010) 'Automatic face annotation in photo collections using context-based unsupervised clustering and face information fusion' IEEE Trans. Circuits Syst. Video Technol Vol. 20 No. 10 pp. 1292–1309

[5] Zou J., Ji Q. and Nagy G. (2007) 'A comparative study of local matching approach for face recognition' IEEE Trans. Image Process Vol. 16 No. 10 pp. 2617–2628

[6] Su Y., Shan S., Chen X., and Gao W. (2009) 'Hierarchical ensemble of global and local classifiers for face recognition' IEEE Trans. Image Process Vol. 18 No. 8 pp. 1885–1896

[7] Xie S., Shan S., Chen X., and Chen J. (2010) 'Fusing local patterns of Gabor magnitude and phase for face recognition' IEEE Trans. Image Process Vol. 19 No. 5 pp. 1349–1361.

[8] Liu C. and Wechsler H. (2002) 'Gabor feature based classification using the enhanced fisher linear discriminant model for face recognition' IEEE Trans. Image Process Vol. 11 No. 4 pp. 467–476

[9] Ahonen T., Hadid A., and Pietikainen M. (2006) 'Face description with local binary pattern: Application to face recognition' IEEE Trans. Pattern Anal. Mach. Intell Vol. 28 No. 12 pp. 2037–2041

[10] Maenpaa T. and Pietikainen M. (2004) 'Classification with color and texture: Jointly or Separately' Pattern Recognit Vol. 37 No. 8 pp. 1629–1640

[11] Paschos G. (2001) 'Perceptually uniform color spaces for color texture analysis: An empirical evaluation' IEEE Trans. Image Process Vol. 10 No. 6 pp. 932–937.

[12] Sim T., Baker S. and Bsat M. (2003) 'The CMU pose, illumination, and expression database' IEEE Trans. Pattern Anal. Mach Intell Vol. 25 No. 12 pp. 1615–1618

[13] Phillips P. J., Moon H., Rizvi S. A., and Rauss P. J. (2000) 'The FERET evaluation methodology for face recognition algorithms' IEEE Trans Pattern Anal Mach Intell Vol. 22 No. 10 pp. 1090–1104

International Journal of Science and Engineering Applications
Volume 2 Issue 4,2013, ISSN-2319-7560 (Online)

Electronic and Spectroscopic Study of the GaAs nitridation – Electronic Characterization Associated

Nacera Bachir Bouiadjra
AMEL, Djillali Liabès university
Sidi Bel Abbès, Algeria

Zineb Benamara
AMEL, Djillali Liabès university
Sidi Bel Abbès, Algeria

Abdelkrim Sellam
IRECOM Laboratory, Djillali Liabès university
Sidi Bel Abbès, Algeria

Luc Bideux
LASMEA, UMR 6602
Avenue des Landais, 63177,
Aubière CEDEX, France

Christine Robert
LASMEA, UMR 6602
Avenue des Landais, 63177,
Aubière CEDEX, France

Bernard Gruzza
LASMEA, UMR 6602
Avenue des Landais, 63177,
Aubière CEDEX, France

Abstract: Gallium nitride is one of the III-V semiconductors the most promising in many application areas. Indeed, because of its large direct bandgap (3,4 eV), it can be dedicated to both optoelectronic applications as transistors achieve hyper frequency. It allows the manufacture of components stable at high temperatures and high frequencies. In this work we are interested in the nitriding of gallium arsenide substrates of n-type in order to obtain a thin layer of GaN. The samples were chemically cleaned immediately introduced into the chamber ultra-high vacuum. They then undergo ionic cleaning in situ by argon ions. Spectrometric analyzes do show the absence of any impurities from the surface, in fact, it only detects the presence of gallium and arsenic. Before proceeding to the nitriding of our structures, deposition of gallium is conducted for 20 minutes to send then simultaneously nitrogen and gallium. Analyzes were performed elaborate structures using X-ray photoelectron spectroscopy (XPS). Deposition of mercury (Hg) has been developed on the structures, we have then made an electrical characterization I-V to see the effect of nitriding on the resulting structure.

Key words: GaAs, GaN, XPS, I-V characterization, Schottky diode.

1. Introduction

A nitridation of GaAs is intensively studied in the last years as the first step of GaN layer deposition or a method for stabilization and passivation of a GaAs surface. Chemical and structural studies on a GaAs surface during and after nitridation.

In this paper, we are interested in the nitridation of GaAs to obtain a Schottky diode rectifier perfectly.

The I-V characteristic shows that our structure are Schottky diode rectifier whose electrical parameters are determined by a fitage of different regions of the characteristic; for our structure, we have determined the values of the series resistance, parallel resistance and the saturation current which are respectively 13Ω, 500Ω et $2{,}5.10^{-6}$ A.

2. Sample Preparation

2.1 Cleaning samples :

The gallium arsenide substrates used were commercial substrates which are in the form of circular plates of thickness of 400 µm and a diameter of about 50 mm. These substrates were made by Czochralski pulling and then cut along the (100) orientation. These samples are doped n-type carrier concentration is $N_d = 1{,}4\times10^{18}$ atomes/cm^3. It is necessary to chemically clean the substrates as they contain various impurities such as oxides and fats.

The samples chemically cleaned were immediately introduced into the chamber ultra-high vacuum. They then undergo ionic cleaning in situ and characterized by photoelectron spectroscopy (XPS). All spectra were performed under excitation with X skate MgKα with energy hν = 1253,6 eV.

To our experience, the ion cleaning with Ar + ions, is carried out with an argon ion kinetic energy of 1 keV, a current density of 3.8 µA/cm^2 beam, argon pressure in the chamber of 4.10^{-5} Torr with a cleaning time of 60 min.

2.2 Study of the evolution of the Ga3d transition

Figures 1 and 2 show respectively the Ga_{3d} transition after chemical cleaning and after cleaning ion respectively. We have broken this transition in a single peak as the difference in energy doublet $Ga_{3d5/2}$ $Ga_{3d3/2}$ related to the spin-orbit coupling is small (0.44 eV) [1, 2, 3]. The peak position associated with the GaAs link is located at 19,2 ± 0,2 eV [4]. As shown in Figure 1, a GaAs substrate, although subjected to chemical cleaning has yet oxides. Indeed, there is a contribution located at 20,4 eV ± 0,2 eV which corresponds to the Ga-O bonds attributed to gallium oxide Ga_2O_3 [4,5]. The analysis also shows that the transition ion bombardment of the substrate does not involve the formation of metallic gallium on the surface. In fact, the Ga_{3d} transition has not a contribution of metalic gallium at 0,7 ± 0,2 eV [4] towards lower bond energies. The parameters of the decomposition peak shape and width at half height of a peak in a given transition, are determined from the decay of the peak in the cleaned substrate. We considered that the width at half height of a transition is independent of the nature of the chemical bond. Note that the peak intensities of photoelectrons are measured relative to a reference sample or placed in the test chamber.

The decomposition parameters of the Ga_{3d} transition are [1] :

- Width at half-height : 1,8 ± 0,2 eV ;

- Peak shape : 20% gaussien – 80% lorentzien.

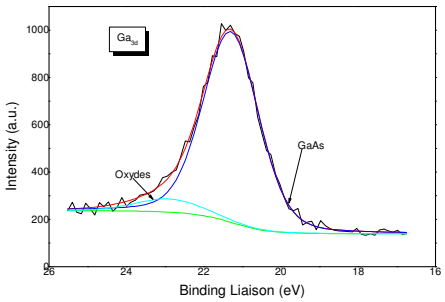

Figure 1: Spectrum of the Ga_{3d} transition after chemical cleaning

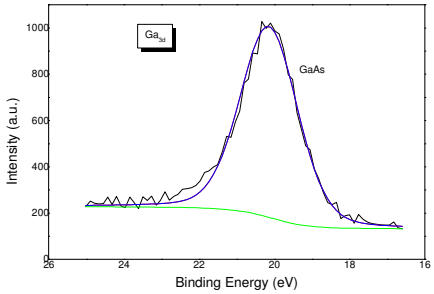

Figure 2: Spectrum of the Ga_{3d} transition after ionic cleaning

2.3 Study of the As3d transition

This transition is shown in Figure 3. It represents the XPS spectrum of the As_{3d} transition cleaning after 60 min with argon ions. It includes only the contribution As-Ga bonds which is located at 40,8 ± 0,2 eV [4, 6]. This contribution is divided into doublet $As_{3d5/2}$ and $As_{3d3/2}$ related to spin-orbit coupling with the gap in the doublet is 0,7 eV and which the area ratio is between 1,2 and 1,4.

The parameters of the decomposition peak shape are [1] :

- Width at half-height : 1,6 ± 0,2 eV ;
- Peak shape : 50% gaussien – 50% lorentzien.

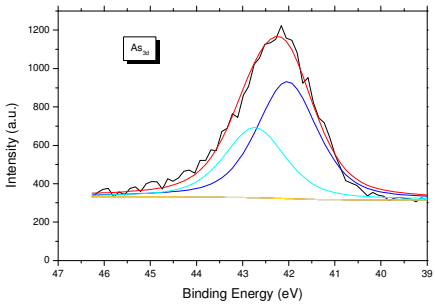

Figure 3: Spectrum of the AS_{3d} transition after ionic cleaning

2.4 Study nitriding substrates

We studied the nitridation of GaAs using as a source of nitrogen production assets, the source type radio-frequency plasma. We prepared samples nitrided at a temperature of 550 ° C and a pressure of 2×10^{-4} Pa.

Figure 4 shows the spectrum of the Ga_{3d} transition after nitriding. This transition has a new contribution at 0,7 ± 0,2 eV towards higher binding energies. It corresponds to the Ga-N bonds[2, 7]. The parameters used for the decomposition Ga_{3d} nitrided were kept identical to those of Ga_{3d} cleaned.

This transition also includes a contribution due to oxides of gallium. The oxidation rate is 13% of the surface of the GaN bonds. This oxidation is attributed to experimental conditions such that the residual pressure of oxygen in the deposition chamber.

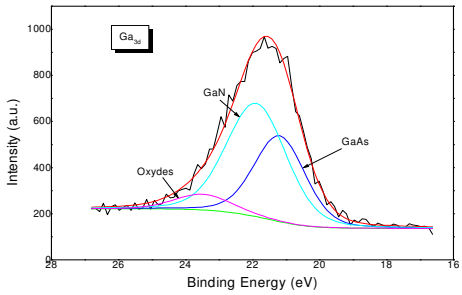

Figure 4: Spectrum of the Ga_{3d} transition after nitridation

Figure 5 shows the N_{1s} transition. It includes a contribution located at 397 eV associated with Ga-N bonds[8] and a contribution located at 2.5 eV to higher energies. This contribution is attributed to bonding states of (N-Ga-O) type content in the nitride film.

The decomposition parameters of the N_{1s} transition are [1] :

- Width at half-height : 2,2 ± 0,2 eV ;
- Peak shape : 50% gaussien – 50% lorentzien.

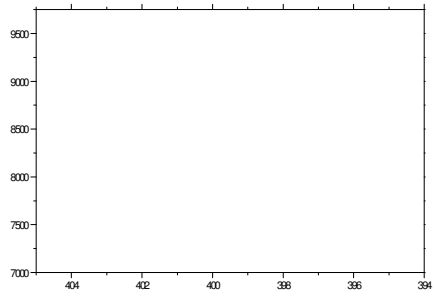

Figure 5: Spectrum of the N_{1S} transition after nitridation

Figure 6 shows the As_{3d} transition. It comprises in addition to the associated pair of links with the substrate, a contribution located at 1,4 ± 0,2 eV, to higher energies. This contribution is probably due to connections arsenic oxides[9].

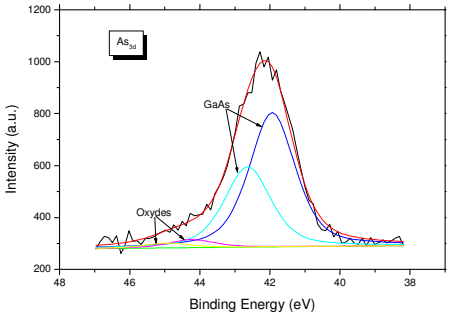

Figure 6: Spectrum of the As_{3d} transition after nitridation

3. Electrical characterization

3.1 Numerical modeling :

The main process of electrical conduction observed in a Schottky diode are :

- The thermionic emission of carriers who can cross the barrier. The expression that connects the current potential applied directly on the diode is [10] :

$$I(V)=I(0)\times\exp\left(\frac{q\times V-R_s\times I}{n\times K_B\times T}\right) \quad (1)$$

Where V is the direct applied bias, n is the ideality factor, Rs is the series resistance of the diode, I(0) is the saturation current.

With ideality factor near 1.

- The recombination of carriers on deep centers generation-recombination. The current follows, again, the law of variation given by equation (1), with ideality factor near 2.
- The tunneling of electrons through the potential barrier of semiconductor to the metal. The tunnel effect can be observed, under direct polarization in the case of a degenerate semiconductor.

The equation of tunnel current is given by the following equation [10] :

$$Itu(V)=Itu(0)\times\exp\left(\frac{V-R_s\times I}{E_0}\right) \quad (2)$$

$$\text{where : } E_0=E_{00}\times\coth\left(\frac{q\times E_{00}}{k_B\times T}\pi\right)$$

$$\text{With : } E_{00}=q\times\frac{\hbar}{2}\sqrt{\frac{N_d}{\varepsilon_0\varepsilon_s m_e^*}}$$

- If there is a highly conductive layer at the metal-semiconductor interface, which is the origin of leakage currents in the diode, the current may be due to the effect of a parallel resistance R_p. The term of this current is [10] :

$$I_{R_P}(V)=\frac{V-R_s\times I}{R_p} \quad (3)$$

This is more likely when the level of reverse current is high enough.

3.2 Electrical measurements

To study the effect of nitriding of electronic devices based on GaAs, I-V characterization was made on nitrided GaAs on GaAs chemically cleaned and non-nitrided. For an electronic device, a ball of mercury is applied onto the two structures. The result of the direct I-V characterization is shown in Figure 7. This figure shows that we have a current gain important for the structure based on GaAs nitrided structure which corresponds to a rectifier. We explain this in that the nitridation of GaAs has the effect of preventing oxidation of the surface. In addition, the GaN layer obtained is very thin (≈ 30Å), so the resulting structure is actually a Schottky diode Hg/GaAs with a GaAs surface treated by nitriding.

Figure 8 shows the direct and reverse I-V characteristic of the Hg/GaN/GaAs structure on a semi-logarithmic scale. This figure shows that the direct characteristic contains two parts corresponding to two different conduction models. For bias voltages greater than 0.55 V, the characteristic is dominated by the series resistance effect with a conduction due to the phenomenon of generation-recombination because the ideality factor is about 2. However, the reverse saturation current, the series resistor, the parallel resistor and the potential barrier height are respectively measured at :

$I_S = 2{,}5.10^{-6}$ A ; Rs = 13 Ω ; Rp = 500 Ω ; Φ_{BN} = 0,63 eV .

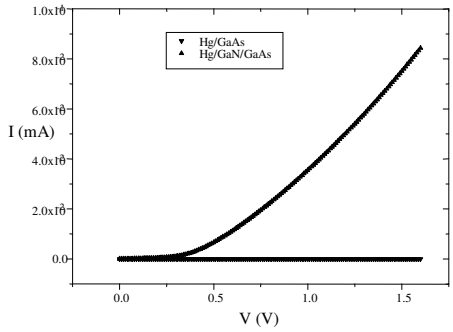

Figure 7: Direct I-V Characteristics for Hg/GaAs and Hg/GaN/GaAs structures

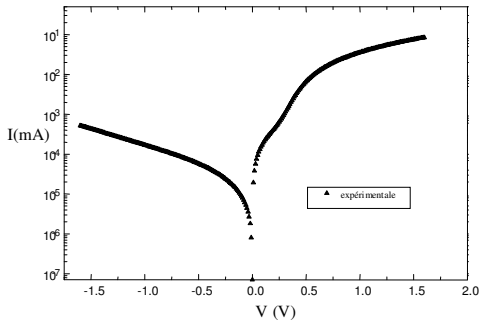

Figure 8: Direct and reverse I-V Characteristic for the Hg/GaN/GaAs structure

4. Conclusion

In this work, we have demonstrated the effectiveness of the process of nitriding of GaAs for obtaining the first GaN layers. We have demonstrated the interest of the photoelectron spectroscopy (XPS) for the control of surface evolution based treatments applied to the surface of the substrates. This

analysis also enables us to know the elements present on the surface as well as the elements which are connected. We noticed that the nitridation of GaAs at the same time causes the oxidation of the surface oxidation that we assigned to experimental conditions such that the residual pressure of oxygen in the deposition chamber.
I-V Electrical measurements on two structures type Hg/GaAs et Hg/GaN/GaAs ; the second structure looks rectifier with high current gain while the first structure did not. We also determine from the I-V characteristic obtained for the structure Hg / GaN / GaAs some electrical parameters of the developed structure.

5. REFERENCES

[1] Y. Ould-Metidji Thèse de Docteur d'Université, Université Blaise Pascal (2002).

[2] L.A. DelouiseJ. Vac. Sci. Technol. A10 (4), (1992). 1637.

[3] L.A. Delouise J. Vac. Sci. Technol. A11 (3), (1993). 609.

[4] J.F. Moulder, W.F. Stickle, P.E. Sobol, K.D. Bomben Hand Book of X-ray Photoelectron Spectroscopy ; Edité par J. Chastain, Publié par Perkin-Elmer corporation (1992)

[5] J.L. Sullivan, W. Yu, S.O. Saied Applied Surface Science. 90 (1992) 515.

[6] Hand Book of X-ray Photoelectron Spectroscopy Edition JEOL (1991).

[7] J.S. Pan, C.H.A. Huan, A.T.S. Wee, H.S. Tan, K.L. Tan J. Mater. Res. 13 (7), (1998) 1799.

[8] P. Hill, J. Lu, L. Haworth, D.I. Westood, J.E. Macdonald Applied Surface Science. 123/124 (1998) 126.

[9] Y. Misokawa, H. Iwasaki, R.Y. Nishitani, S. Nakamura J. of Electron Spectroscopy and Related Phenomena. 14 (1978) 129.

[10] A.M.J.F. Philippe Thèse de Docteur d'Université, Institut National des Sciences de Lyon (1999).

International Journal of Science and Engineering Applications
Volume 2 Issue 4, 2013, ISSN-2319-7560 (Online)

AUTOMATIC SEGMENTATION MYOCARDIAC IMAGES USING MAXIMUM ENTROPY

Mr.Yogesh pawar
Prof MIT AOE,
Alandi, Pune, India

Sahil Dhammani
MIT AOE,
Alandi, Pune,India

Dnyaneshwar Wable
MIT AOE,
Alandi, Pune,India

Mukund Baheti
MIT AOE,
Alandi,Pune,India

Abstract: The digital image processing is a widespread applicable technique especially in the area where tools are used for feature extraction and to obtain patterns of studied images. Initially segmentation is used to separate the image into parts that represent an interest object that can be used for further specific study. There are various techniques present which performs such task but a common technique that adapt to all images is required, especially for complex or specific images. Hence our project basically aims to obtain a technique which is convenient for complex and different images. We tend to obtain a more specific result of the input image using histogram quantization, calculating valleys from analysis of histogram slope percentage, calculating threshold using maximum entropy.
This approach provides more specific results over the already proposed technique which will be of great importance to the doctors, pathologists and surgeons to detect the potential cell rejection.

Keywords: thresholding, maximum entropy, segmentation, valleys, histogram.

1. INTRODUCTION

The goal of segmentation is to simplify and/or change the representation of an image into something that is more meaningful and easier to analyze. The simplest method of image segmentation is called the thresholding method. This method is based on a clip-level (or a threshold value) to turn a gray-scale image into a binary image. In image processing, thresholding is most common method in extracting objects from a picture. If a object is clearly distinguishable from its back ground the gray level histogram will be bimodal and threshold for segmentation can be chosen at bottom of valley. But gray-level histogram is not always bimodal. Methods other than valley seeking are requires to solve this problem.

The key of the method is to select the threshold value (or values when multiple-levels are selected). Several popular methods are used in industry including the Otsu's method (maximum variance), and k-means clustering for detection of threshold.

Histogram based methods are very efficiently when compared to other image segmentation methods because they typically require only one pass through the pixels. In this technique, a histogram is computed from all of the pixels in the image, and the peaks and valleys in the histogram are used to locate the clusters in the image.

The techniques used till dates do not provide a good threshold values that would provide segmentation of entire image. Previous technique proposed a methodology where the algorithm automatically gets the multilevel threshold, by the histogram analysis [1]. The method finds the histogram valleys, which are the places where are concentrated the thresholds and therefore the subdivision of the image. However the method proves effective in cases where the image and the histogram are well defined, for cases where the image is not presented optimally, with noise, distortion and no standardized histograms, the method does not produce an effective threshold that identifies the objects in the image quality. In this context, the paper presents an improved version of the model of multilevel automatic thresholding described in previous methods, considering the group histogram quantization, analysis of the histogram slope percentage and calculation of maximum entropy to define the threshold. These improvements prevent the identification of not significant thresholds and allow more control of the technique during the step of feature extraction in artificial vision systems.

2. METHODOLOGY

Histogram-based methods are very efficient when compared to other image segmentation methods because they typically require only one pass through the pixels. In this technique, a histogram is computed from all of the pixels in the image, and the peaks and valleys in the histogram are used to locate the clusters in the image.

The automatic multilevel thresholding method determines the threshold based on the identification of Maximum entropy by comparing the entropies in different regions of the histogram of the image in question. This method is an improvement which allows better control over the thresholds identified [1]. For such, properties were added to the method cited, such as the division of the histogram into classes, analysis of the slope percentages and the determination of the threshold by the calculation of maximum entropy.

The first step in segmentation is to determine the histogram of the image to be studied. The histogram is then divided into classes. A class is one or more gray scale values that make up the histogram. For this division, it is necessary to predefine the class size. If the value informed is 1, the process analyzes

each of the intensities of the histogram. For values greater than 1, the increment considered in the iteration process of the method is the predefined value. For instance, consider a class made up of 10 intensities and a histogram with 256 gray levels. The first class encompasses levels 0 to 9, the second encompasses 10 to 19, and so forth, totaling 25 classes will 10 levels of gray and one class with six levels (figure 1).

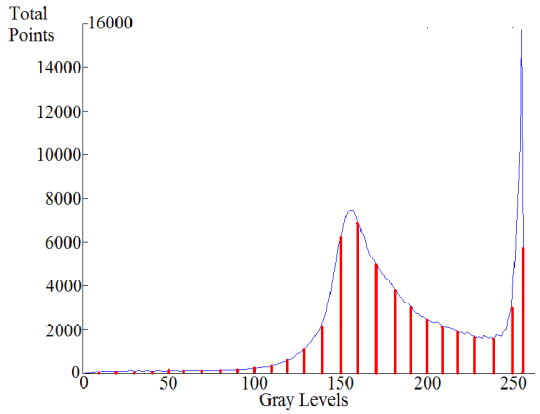

Figure. 1 Example of histogram divided into 26 classes – 25 containing 10 levels and one containing six levels; vertical lines demark classes

Now identify what classes have valleys that are relevant to the specification of the thresholds. The method automatically identifies these classes by means of sign
Transition, analyzing the following characteristics:
• The mean of the points contained in the first half of the class analyzed is compared with the mean of the points in the second half of the same class. If the value of the first half is smaller, the values of the histogram are increasing toward a peak and the sign attributed to the class is positive. Otherwise, a negative sign is attributed to the class, indicating movement toward a valley.
• The sign of the next class is determined. If there is a transition from a negative to a positive sign, the valley is relevant to the specification of a threshold (figure 2).

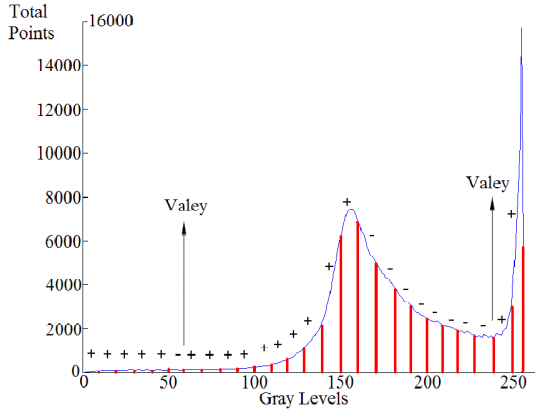

Figure 2. Example of histogram divided into 26 classes with indication of two relevant Valleys to the determination of thresholds – one at level 50-59 and another at level 230-239.

The determination of thresholds based on valley analysis may be influenced by homogeneous regions in the histogram (with no valleys or with non-significant valleys). To solve this problem, the proposed method determines that a class is relevant if it has a slope percentage greater than a predefined value. This value can be adjusted to the type of image being studied. A slope percentage is the percentage difference between the means of the points in the first and second halves of the class being analyzed. Two or more classes are grouped together when the slope percentage is lower than the predefined value. This resource allows controlling the sensitivity of the method. A threshold is established when the slope percentage of the class is greater than the predefined value. In the study of images of myocardial biopsies of transplant patients, the values used for the input parameters for segmentation were classes of size 10 and the slope was defined at 35%. These values proved sufficient for the appropriate segmentation of the regions of interest.

Threshold identification using maximum entropy. For each relevant class identified to define a valley, a threshold is calculated based on entropy, considering a probability of an intensity correctly segmenting a given group of objects. For such, the image is taken as the result of a random process in which probability p corresponds to the probability of a pixel in the image taking on an intensity value $i(i=1,..,n)$ [3], as shown in equations below. The intensity or gray level of the class with the greatest entropy is identified as a threshold.

$$H = -\sum_{i=1}^{n} p_i \log(p_i)$$

$$p_i = \frac{n_i}{N}$$

in which H is the entropy of the image; n is the total number of outputs (number of gray levels in the image); pi is the probability of gray level i being found in the image; ni is the number of pixels with intensity i; and N is the total number of pixels in the image. The gray level of the group indicated with the highest entropy is identified as a threshold. Completed this phase, the process continues with the analysis of the other groups. To test the technique, we used myocardial images of biopsies from heart transplant. The choice of this type of image to processing is justified by the groups of existing objects, cell core, fibrous tissue, muscle and tissue rejection. 120 images were processed and the results were compared with those provided by the technique presented in Otsu's method.

3. RESULTS

In the studied images we used four different input parameters, the image format to be processed, the size of the histogram division group, the filter size, and the percentage of slope to be used for identify thresholds.

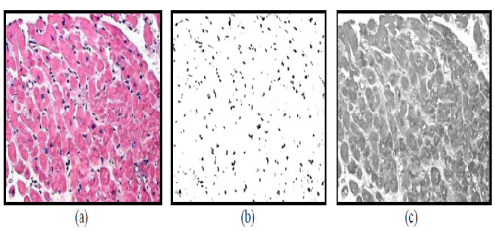

Figure 3: Illustrative case of image obtained from myocardial biopsy of heart-transplant patient
(a) prior to processing; (b) result obtained with proposed segmentation method revealing cell nuclei
and (c) heart muscle (gray) and interstitial spaces (white).

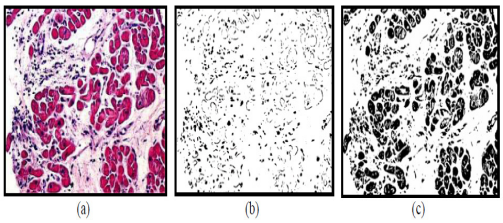

Figure 4: (a) myocardial biopsy classified as 2R used to illustrate visual differences obtained with different segmentation methods; (b) cell nuclei segmented using proposed method and (c) using
Otsu's method [2].

.

4. REFERENCES

[1] S. R. Aboud Neta, L. V. Dutra, G. J. Erthal1, "Limiarização automática em histogramas ultimodais". Proceeedings of the 7th Brazilian Conference on Dynamics, Control and Applications, FCT – Unesp de Presidente Prudente, May, 2008.

[2] Otsu N A 1979 Threshold selection method from gray-level histogram IEEE Transactions on

[3] Pun T 1980 A New Method for Gray-Level Picture Thresholding Using the Entropy of the

International Journal of Science and Engineering Applications
Volume 2 Issue 4, 2013, ISSN-2319-7560 (Online)

Automated Drilling Machine with Depth Controllability

G.Niranjan
Dept. of Electronics & Communication Engineering
Aurora's Technological & Research Institute
Hyderabad, India

A.Chandini
Dept. of Electronics & Communication Engineering
Aurora's Technological & Research Institute
Hyderabad, India

P.Mamatha
Dept. of Electronics & Communication Engineering
Aurora's Technological & Research Institute
Hyderabad, India

Abstract: Estimating the drilling depth while drilling manually through a conventional drilling machine is extremely impossible, often the job will be failed due to the over drilling. In many cases, after completing the drilling work, it is very difficult to measure the depth; especially thin holes depth can't be measured. Therefore an automatic drilling machine that performs the function of drilling according to the drilling depth generated & forwarded to the control circuit is essential; hence this project work is taken up, which exposes the technology of special purpose drilling machines.

The Electrical drilling machine designed here is quite useful for mechanical workshops. The machine is constructed with power feed technology is aimed to drill the job up to certain specified depth, For ex: if a particular piece of job is supposed to be drilled to a limited depth, doing it manually consumes lot of time, because every time depth has to be measured through a crude method, thus estimating the drilling depth is quite complicated. For this reason this machine is designed &its mechanical movements are restricted by programming the drilling depth through a potentiometer interfaced with microcontroller.

Keywords: Mechatronics, Limit switch, Motor shaft, Mechanical transmission section, Depth control mechanism.

1. INTRODUCTION

Simple drilling machines like hand held portable drilling machines, power feed drilling machines, etc. are quite common, we can find these machines everywhere. Often these machines are used for drilling a through hole over the job; these machines cannot be used for number of machining operations for specific applications. Human force is required to drill the hole, drilling depth cannot be estimated properly, job may spoil due to human errors, and different size holes cannot be drilled without changing the drill bit. Consumes lot of time for doing repeated multiple jobs, these all are the drawbacks. To overcome all these problems, this automated drilling machine is designed which is aimed to drill the holes automatically over a job according to the drilling depth data programmed through a key board. According to our survey report, we came to know that the machine designed here with a drilling machine is quite new, & there is no substitute available in the market.

The main concept of this machine is to drill the holes over particular jobs repeatedly at different depths, sequence is maintained. As the machine contains drill motor, the movement is controlled accurately. The mechanical transmission section is controlled with stepper motor, based on the drilling depth programmed through keyboard; the microcontroller restricts the movements of drill motor through stepper motor. Entire process falls under the subject of Mechatronics, & various fields of technologies must be included to full-fill the target. The integration of electronic engineering, mechanical engineering, electrical engineering, & control technology is forming a crucial part in this design. Especially the control circuit designed with microcontroller plays dominant role in this project work.

2. BLOCK DIAGRAM & ITS DESCRIPTION

The main concept of this project work is to design & develop one special purpose-drilling machine, which can be used to drill the job with different depths programmed independently. These kinds of drill machines are very much required in the mechanical workshops, where it is essential for specific job applications. Drilling depth of the motor can be programmed through the potentiometer. The drilling motor is moved in vertical direction through power feed technology designed with stepper motor. The stepper motor used to move the drilling motor upward & downward directions is aimed to pull down the drill motor while drilling the hole over the job. Here some force is applied such that the machine can be able to drill the hole over light metal jobs. Since the project work is considered as prototype module, the stepper motor used here can apply a little force. To drill over heavy metals like MS, high power motor with suitable gear mechanism is essential.

The main purpose of this machine is to control the drilling depth accurately; therefore the control circuit should able to recognize the target entered through potentiometer. In this regard, the vertical moving mechanism is coupled to the stepper motor shaft, as this motor rotates step wise & step angle is 1.8^{o}, the movement of mechanism per step can be measured. Each pulse produced by the controller can rotate the motor by one step, since step angle is 1.8^{o}, 200 pulses are required to rotate the motor for one full revolution. When the stepper motor completes one full revolution, initially movement in the vertical mechanism must be measured with the scale. Based on this data the controller can be programmed through keyboard. For example, if the power feed motor (stepper motor) completes one revolution assume that the mechanism is moved by 1mm down, to move the mechanism by 1mm the controller has to produce 200 pulses. Now the controller can recognize the movement of mechanism by counting the pulses internally. The entire vertical moving mechanism that contains drilling motor is coupled with power feed motor can be called as depth control mechanism.

The depth control mechanism coupled to the drilling machine can be used for drilling to a desired depth; the desired depth can be programmed through a potentiometer interfaced with controller chip. This technology prevents the twist drill from traveling too far after cutting through the work piece. The depth control mechanism was designed to be used whenever a number of holes of the same depth are to be drilled, or when drilling holes deep into the work piece. Make sure that drills are chucked tightly to avoid slipping and changing the depth setting. Most depth stops have a way to measure the distance that the drill travels. Some may have a fractional gage on the depth stop rod, and some may have a micrometer dial located on the depth stop for very precise measurements. But here in this concept depth control machine can be programmed such that no tool is required for measuring the depth. Once it is aligned, it can be used for mass production.

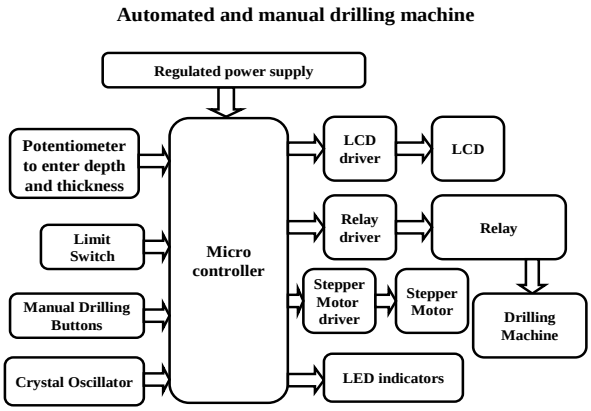

Figure 1. Block Diagram

3. CIRCUIT DIAGRAM & ITS DESCRIPTION

The project "Automated Drilling Machine with Depth Controllability" using PIC microcontroller is an exclusive project which is used for automatic control over drilling depth by a microcontroller based system. According to the program dumped onto the microcontroller, the drilling machine, stepper motor and other devices starts working to obtain the successful output. When the power is supplied to the setup, the 230V supply is converted to constant 5V and then supplied to the microcontroller and its components. With the help of a potentiometer the inputs (i.e., depth of the hole to be drilled & thickness of the object) are given. The display section is designed to display the drilling depth data of the drilling motor. For this purpose an LCD panel is used & it is interfaced with microcontroller through its output port. This display is having two rows & each row can display 16 characters. The drilling depth data of the motor is entered in mm through the potentiometer, & is displayed on the LCD.

Relay is an electrically operated switch that is used to drive the ac devices (drilling machine).

The most important electrical device used in the project work is Stepper motor. In a stepper motor, the electromagnets are energized by an external control circuit, such as a microcontroller. To make the motor shaft turn, first one electromagnet is given power, which makes the gear's teeth magnetically attracted to the electromagnet's teeth. When the gear's teeth are thus aligned to the first electromagnet, they are slightly offset from the next electromagnet. So when the next electromagnet is turned on and the first is turned off, the gear rotates slightly to align with the next one, and from there the process is repeated. Each of those slight rotations is called a "step," with an integer number of steps making a full rotation. In that way, the motor can be turned by a precise angle. Stepper motors are ideally suited for precise positioning of an object or precise control of speed without having to resort to closed loop feedback. These motors rotate in step-wise i.e., this stepper motor rotates a precise angular distance, one step for each pulse that is delivered to its drive circuit. The motor used in this project work has a step angle of 1.8^0 per pulse. In order to rotate the motor shaft for one complete revolution i.e., 360^0, it is required to supply 200 pulses ($360 / 1.8^0 = 200$) to the motor's drive circuit. This drive circuit is then connected to drilling machine, which is the main device of the project. Drilling machine rotation & movement is based on the stepper motor rotations.

For identifying the home position of the drilling machine & to restrict the vertical movement at top position, limit switch is arranged to the structure. This switch is interfaced with microcontroller as input signal. This limit switch is having long lever & when little pressure is applied to the lever, switch will be activated automatically. The mechanical transmission section that carries the drill motor activates the switch at home position. Whenever the limit switch is activated, active low signal will be generated, based on this signal the microcontroller can recognize the position of drill motor. Thus the power can be saved to a maximum extent.

In this project based on thickness & depth entered, the drilling machine drills the hole into the object that is placed under the drill-bit. Thus the desired hole of desired depth is obtained, hence the name "Automated Drilling Machine with Depth Controllability".

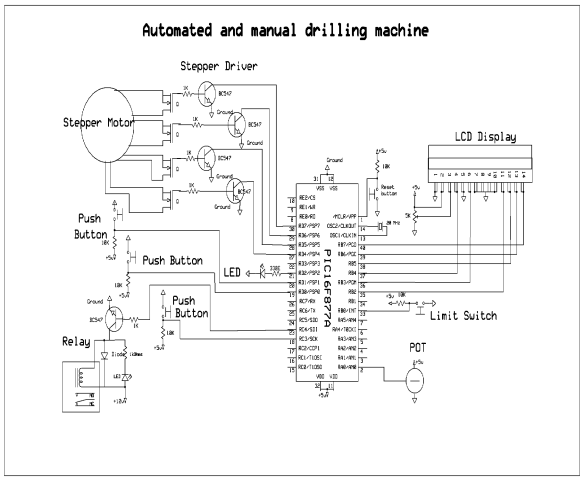

Figure 2. Schematic Diagram

4. RESULT

The project "**Automated drilling machine with depth controllability**" was designed such that the drilling depth is controlled automatically to set value by microcontroller based system.

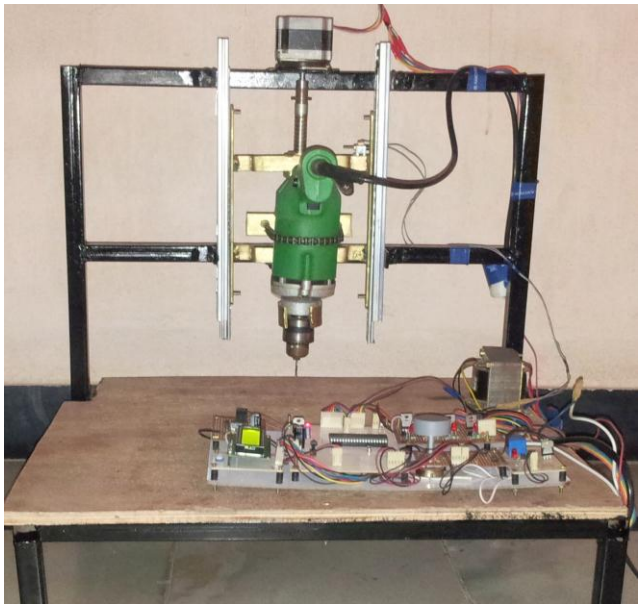

Figure 3. Automated & Programmed Drilling Machine

5. CONCLUSION

Integrating features of all the hardware components used have been developed in it. Presence of every module has been reasoned out and placed carefully, thus contributing to the best working of the unit. Secondly, using highly advanced IC's with the help of growing technology, the project has been

successfully implemented. Thus the project has been successfully designed and tested.

6. ACKNOWLEDGMENTS

We are thankful to our project co-ordinator **Mrs. Y.NAGA SUPRAJA** for her support and valuable suggestions throughout the project research. We are thankful to our project guide **Mrs. P.MAMATHA** for her continuous effort in the fulfillment and guiding us in successful completion of the project research. We are thankful to **Mr. N.D.GHOSH** Sir for his consistent and constant support, encouragement and motivation for the successful completion of the project research. We are thankful to all the above people and our team for completing the project.

7. REFERENCES

[1] Mechatronics and Measurement Systems By: David g. Alciatore, Michael B. Histand

[2] Mechatronics – Electronic Control Systems in Mechanical and Electrical Engineering By: W. Bolton

[3] Introduction to Robotics By Saeed B. Niku

[4] The 8051 Micro-controller Architecture, programming & Applications By: Kenneth J. Ayala

[5] Mechanism and Machine Theory By: J.S. Rao, R.V. Dukkipati

[6] Practical transistor circuit design and analysis-By: GERALD E. WILLIAMS

[7] Robotic Engineering An Integrated Approach By: Richard D. Klafter, Thomas A. Chmiclewski, and Michael Negin

[8] Programming and Customizing the 8051 Micro-controller By: Myke Predko

[9] The concepts and Features of Micro-controllers By: Raj Kamal

[10] Digital and Analog Communication System By: K. Sam Shanmugam

[11] Raj kamal –Microcontrollers Architecture, Programming, Interfacing and System Design.

[12] Mazidi –Embedded Systems.

[13] PCB Design Tutorial –David.L.Jones.

[14] PIC Microcontroller Manual – Microchip.

[15] Embedded C –Michael.J.Pont